63-3-6

Ford Motor Company
AERONUTRONIC DIVISION

Ford Motor Company
AERONUTRONIC DIVISION

Publication No. U-2148

RESEARCH LABORATORY

TECHNICAL REPORT

CHEMICAL CORROSION OF ROCKET LINER MATERIALS AND PROPELLANT PERFORMANCE STUDIES

Fourth Quarterly Technical Summary Report

Prepared for: Advanced Research Projects Agency
The Pentagon
Washington 25, D. C.

Under Contract: NOw 61-0905-c, Task E
With the Bureau of Naval Weapons
ARPA Order No. 22-62

Prepared by: R. C. Oliver
R. W. Baier
D. L. Peters
R. W. Sprague

15 June 1963

ABSTRACT

Studies on the theoretical equilibria resulting from interaction of candidate refractory nozzle wall materials with various chemical species resulting from combustion of rocket fuels have continued. Tantalum carbide has been considered in detail, with composition diagrams and saturation parameters reported for its interaction at 1000 psia with AlF_3, BF_2, BF_3, BOF, BeF_2, CO, CO_2, HCl, HF, H_2, H_2O, LiF and N_2. Similar computations are reported for tungsten interacting with BOF, CO, and CO_2, these results representing a revision of data reported in the previous quarterly report under this contract, as necessitated by a recent revision in the thermodynamic data for the tungsten oxides. The oxides are considered briefly as a class for application in oxygen-containing atmospheres, with results given for MgO, HfO_2 and ThO_2 in CO_2. The stability of carbides in nitrogen is also considered.

The possibility of extending the isothermal saturation results for pure components at 1000 psia to mixtures at other pressures has been considered in some detail, with results that look promising except where multi-atomic species are important which are not considered in the individual cases (e.g., HCN is important in a N_2-H_2 mixture in equilibrium with graphite, but is not considered with the individual pure reactants). A "catalog" of ablation reactions for studies reported previously is included.

Plans for future work are described briefly. Certain errata for previous reports are appended.

TABLE OF CONTENTS

FIGURES

TABLES

SECTION 1

INTRODUCTION

This is the fourth quarterly report in a program which has two parts, the first being the theoretical appraisal of various refractory rocket liner materials from a chemical standpoint and the second being the computation of theoretical performance of certain rocket propellant combinations. Work in this past quarter has been concerned only with the evaluation of refractory nozzle materials.

Refractory materials under study include graphite, tungsten, and various high melting carbides, nitrides, borides, and oxides. The procedure in use for comparing these materials is to compute the theoretical amounts of these refractory materials required to "saturate" a unit mass of reacting gas or solid which represents a component of a rocket combustion stream; the details of the procedure were given in the Volume I of the Second Quarterly Report[1]. As explained therein, stability is expressed in terms of both an isothermal saturation parameter (the value "A") and an adiabatic saturation parameter (the value "B"). The adiabatic saturation parameter is proportional under certain conditions to the rate of attack by a flowing stream. Both parameters include effects of simple vaporization, which factor becomes important[2] even in the absence of chemical reactions at temperatures greater than about 3500°K, especially with low molecular weight gas streams and with more volatile refractories. The computational technique is arbitrarily extended to temperatures above the melting point without modification, a technique which is valid in terms of chemical stability but obviously not significant in terms of physical stability.

Thermochemical data used in these calculations have been obtained for the most part from the JANAF[3] compilations. It has in addition been necessary to accumulate thermodynamic data for certain heavy metal species not available in these tables, and this has been, prior to this quarter, represented a significant portion of the effort in this program.

Chemical compatibility studies are reported herein for tantalum carbide with various pure gases and solids, and for tungsten in oxygen-containing gases (with the exception of H_2O). In addition oxides as a class are discussed briefly for application in oxidizing atmospheres, as well as nitride-carbide equilibrium. The tungsten-oxygen calculations represent a revision of results reported previously[2], necessitated by recent revisions in the JANAF tabulations of data for tungsten oxides. Equilibrium systems in which $H_2WO_4(g)$ may appear have not been reported, as revision of $H_2WO_4(g)$ thermodynamic data is expected in the near future[4].

The use of an averaging technique to predict the "A" saturation parameter for real combustion gas mixtures is discussed.

SECTION 2

CHEMICAL CORROSION STUDIES

2.1 CHEMICAL CORROSION OF TANTALUM CARBIDE

2.1.1 GENERAL

The chemical stability of tantalum carbide in fourteen different atmospheres was calculated as described in previous reports[1,2] under equilibrium conditions at 1000 psia and various temperatures; the atmospheres were formed by equilibration of the nominal species AlF_3, BF_3, BF_2, BOF, BeF_2, CO_2, CO, HCl, HF, H_2, H_2O, LiF and N_2. (The nominal species specifies the overall stoichiometry; the species itself may, however, be largely dissociated at the temperature and pressure under consideration.) The results are presented as "A" and "B" plots in Figure 1; equilibrium compositions are given in Figures 2 through 6. Principal species contributing to corrosion are shown in Table I.

It is apparent from Figure 1 that in many cases TaC is severely attacked (B values greater than unity) by species containing "loosely" bound oxygen, such as CO_2 and H_2O; species such as BF_3 and BeF_2 which contain "excess" fluorine are less damaging. Exothermic effects are noted for the species HCl, HF and N_2, and endothermic effects with AlF_3, BF_3, BF_2 and BOF.

The species HBO_2 was considered but again gave rather meaningless results as no gas phase was found to be present below about 4500-5000°K, (as

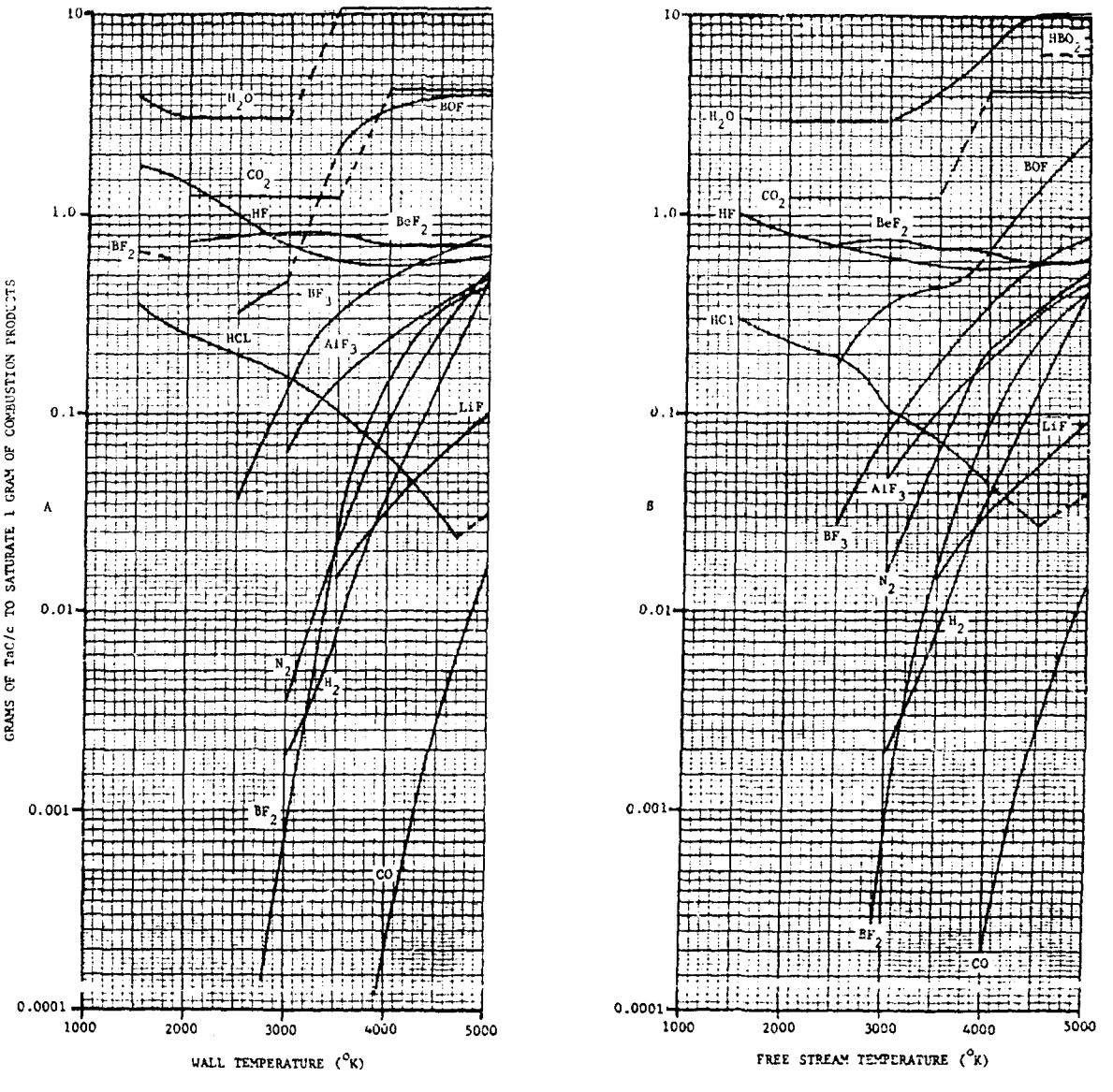

FIGURE 1. CHEMICAL CORROSION OF TaC BY COMMON COMBUSTION PRODUCTS AT 1000 PSIA

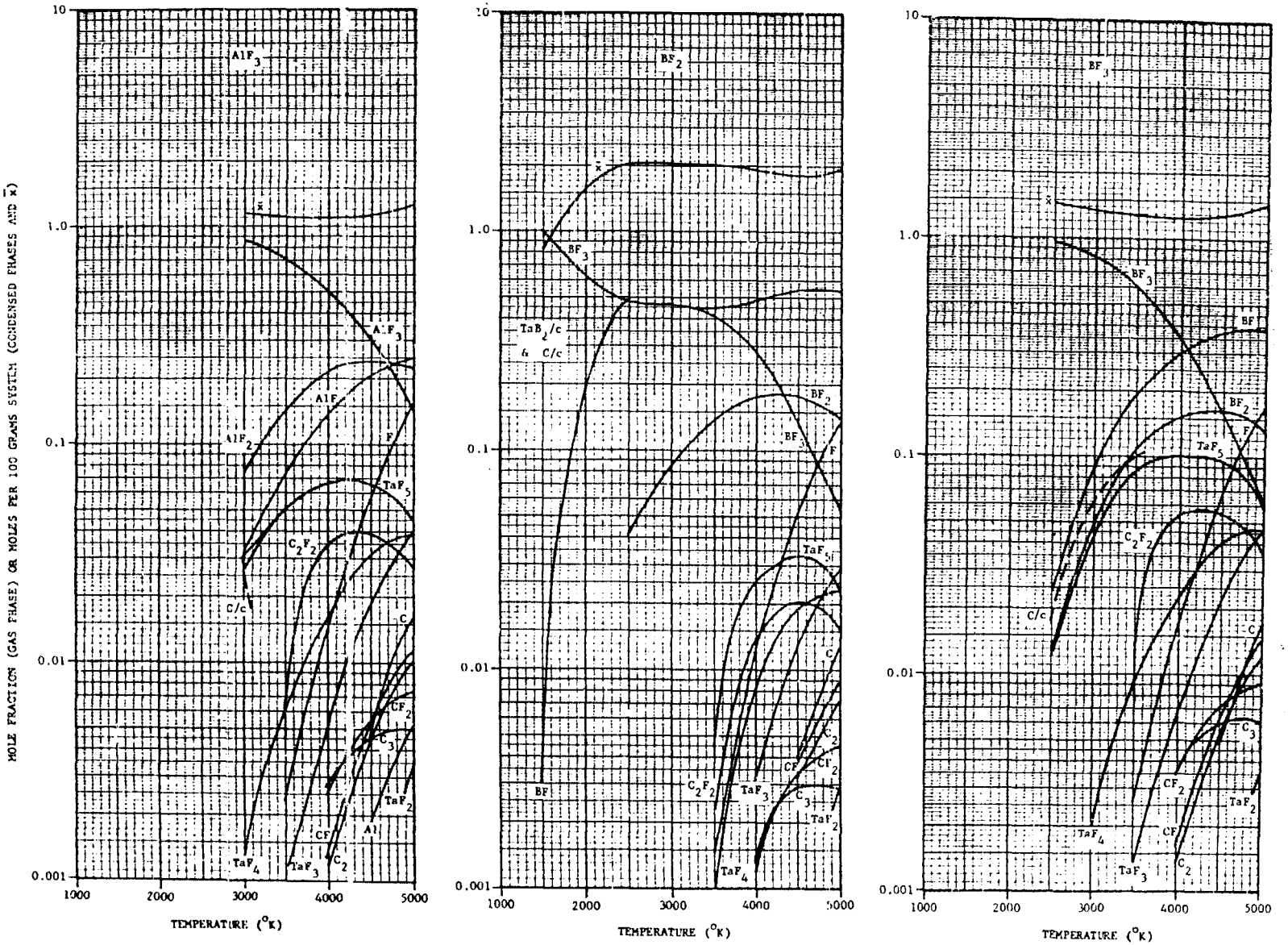

R00114

FIGURE 2. SPECIES PRESENT UNDER EQUILIBRIUM CONDITIONS AT 1000 PSIA FOR TaC AND AlF_3, BF_2, AND BF_3

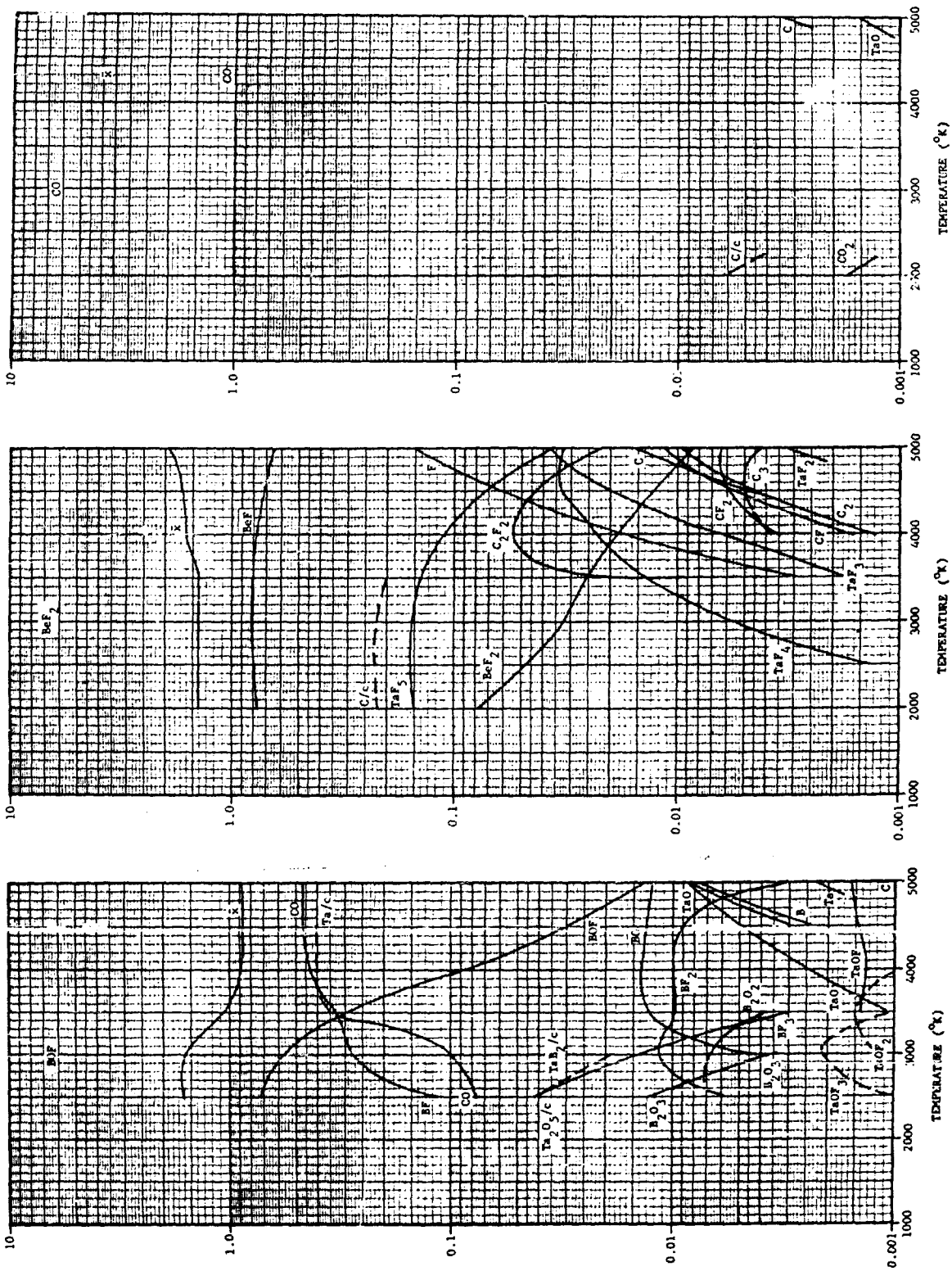

FIGURE 3. SPECIES PRESENT UNDER EQUILIBRIUM CONDITIONS AT 1000 PSIA FOR TaC AND BOF, BeF_2, AND CO

RU0115

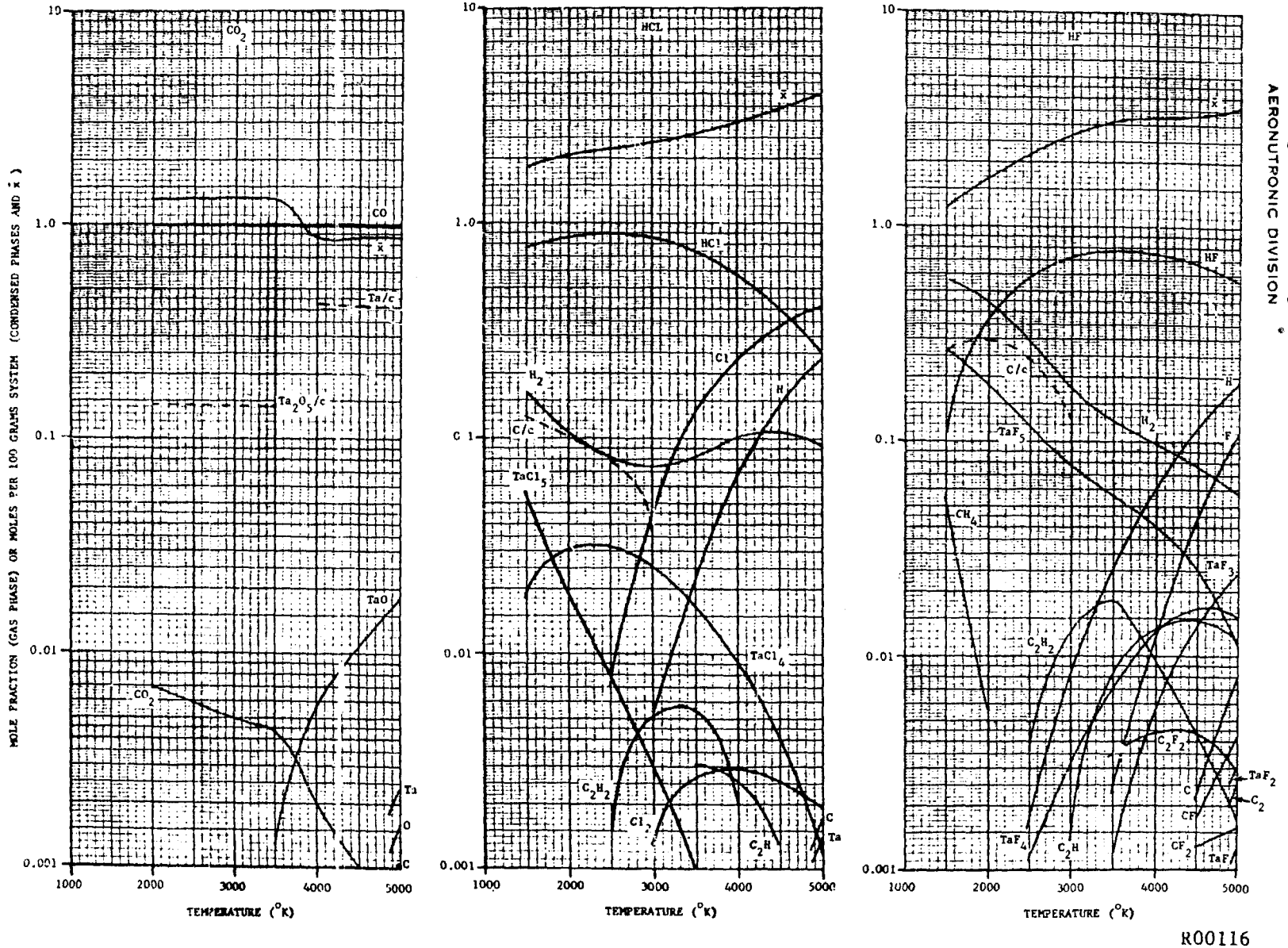

R00116

FIGURE 4. SPECIES PRESENT UNDER EQUILIBRIUM CONDITIONS AT 1000 PSIA FOR TaC AND CO_2, HCl, AND HF

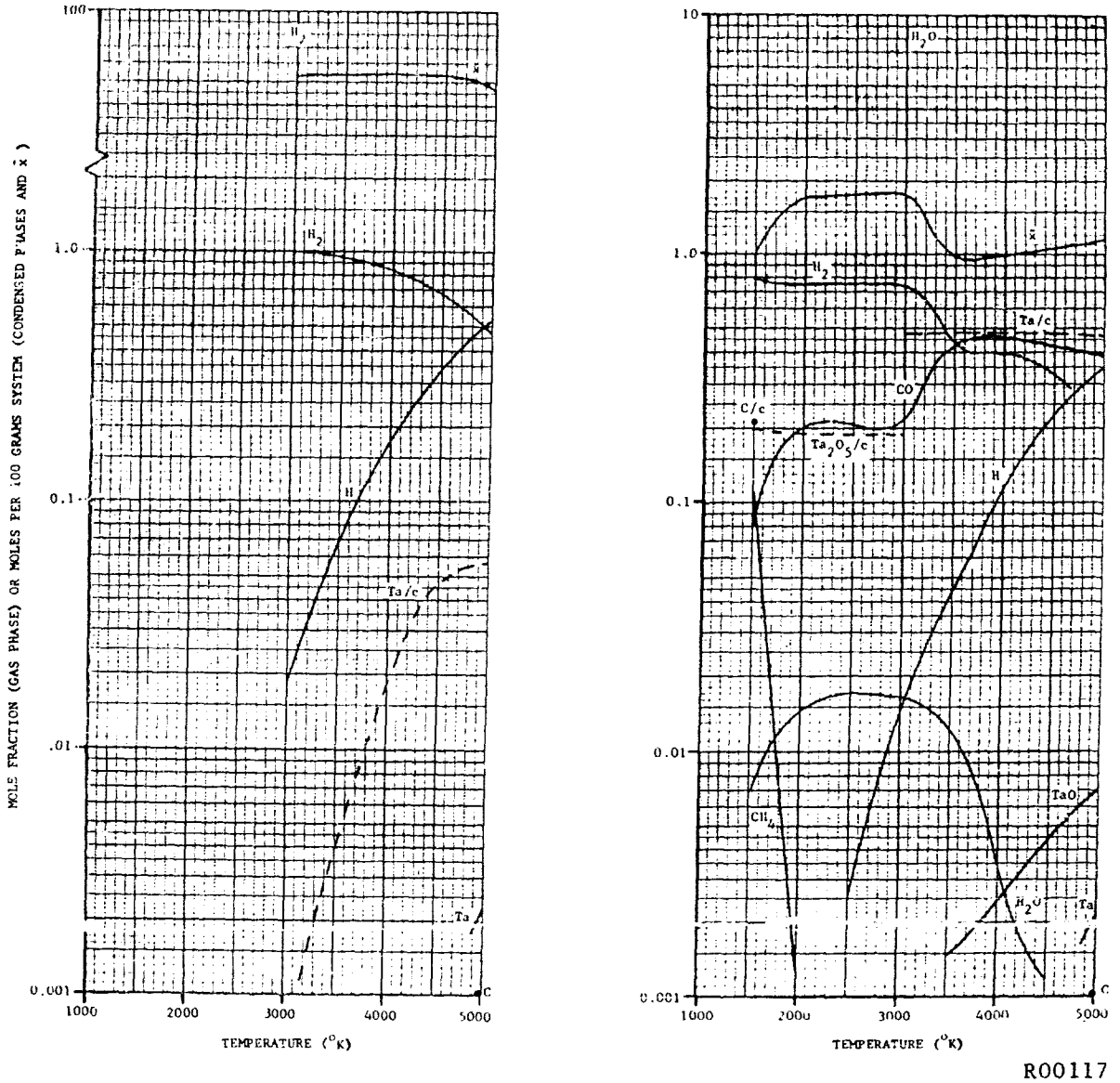

R00117

FIGURE 5. SPECIES PRESENT UNDER EQUILIBRIUM CONDITIONS AT 1000 PSIA FOR TaC AND H_2 AND H_2O

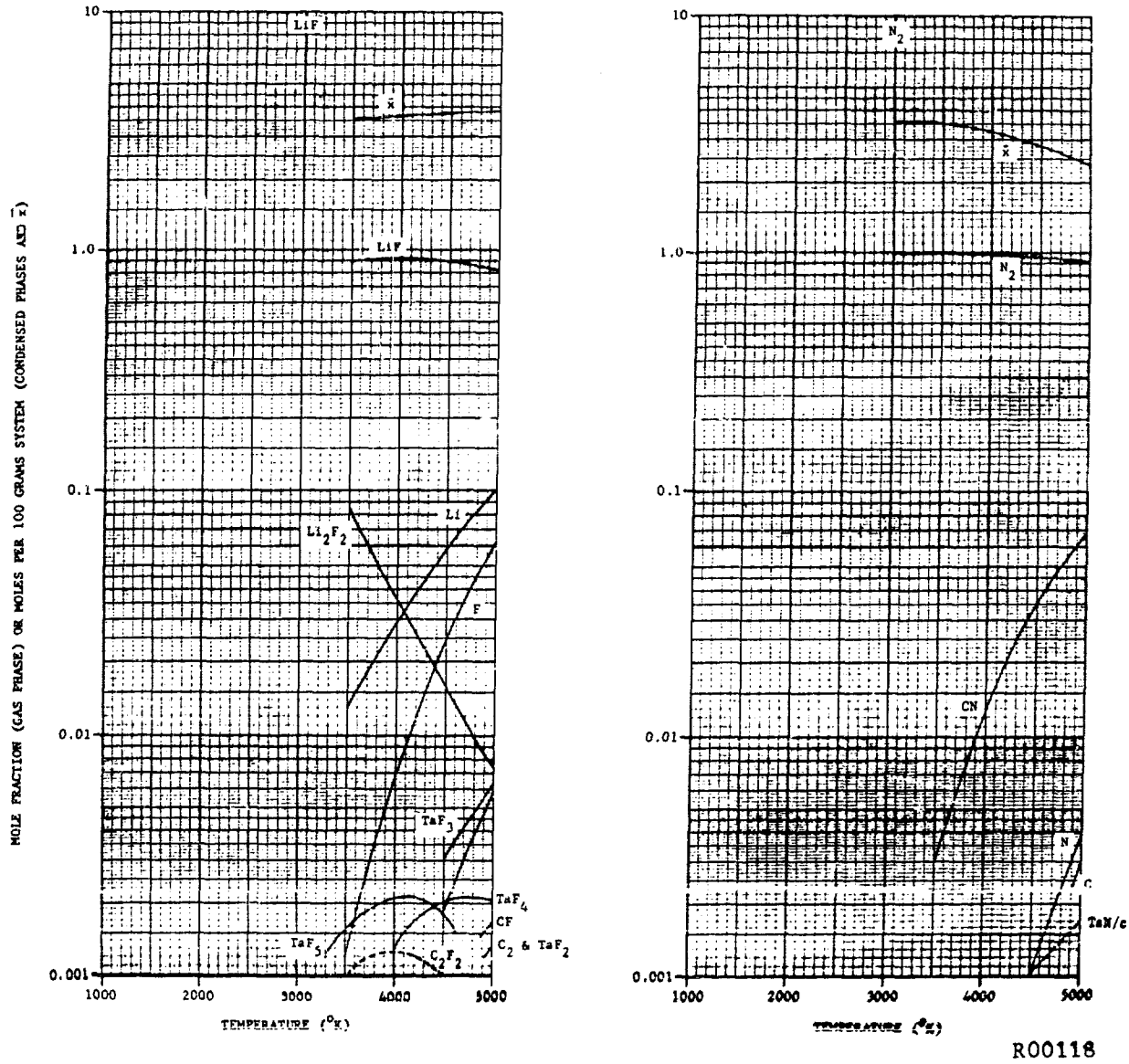

FIGURE 6. SPECIES PRESENT UNDER EQUILIBRIUM CONDITIONS AT 1000 PSIA FOR TaC AND LiF AND N_2

TABLE I

PRINCIPAL SPECIES CONTRIBUTING TO THE ABLATION OF TANTALUM CARBIDE AT 1000 PSIA

Combustion Product	Principal Species at the Nozzle Wall	Approximate Temperature Range($^{\circ}$K)	Remarks
AlF_3	TaF_5, C(c), C_2F_2	3000-5000	No gas phase below about 3000°K.
BF_2	TaB_2(c), C(c)	1500	
	TaF_5, TaF_4, TaF_3, C_2F_2, C	3500-5000	
BF_3	TaF_5, C(c), C_2F_2, TaF_4, TaF_3	2500-5000	
BOF	Ta(c), CO	3500-5000	
	Ta_2O_5(c), TaB_2(c)	2500-3000	
BeF_2	C(c), TaF_5, TaF_4, TaF_3, C_2F_2	2000-5000	
CO	TaO	4500-5000	
CO_2	Ta_2O_5(c)	2000-3500	
	Ta(c), TaO	4000-5000	
HCl	C(c)	1500-3000	
	$TaCl_4$, $TaCl_5$	2000-5000	Decrease with temp.
HF	C(c), TaF_5	1500-5000	Decrease with temp.
	TaF_3, TaF_4, C_2H	3000-4500	Increase with temp.
H_2	Ta(c)	3000-5000	
H_2O	C(c), Ta_2O_5(c), Ta(c)	1500-3000-5000	Solids exist in three separate temp. ranges
	CO	1500-5000	
LiF	TaF_3, C	4500-5000	
N_2	CN, TaN(c)	3500-5000	

was the case with tungsten[2]) and this result was considered unreliable in view of the lengthy extrapolation used in preparing the thermodynamic tables for this species in this region. It accordingly has not been reported in detail.

2.1.2 DISCUSSION OF INDIVIDUAL CASES

AlF_3

The saturation numbers increase over the temperature range investigated, with a fairly constant cooling of about 200°. The cooling can be attributed to endothermic reactions involving formation of tantalum and carbon fluorides.

BF_2 and BF_3

The general behavior of these systems is similar to the AlF_3 system. Cooling is slightly greater in the case of BF_3.

BOF

This system forms solid phases which have a vapor pressure less than 1000 psia below about 2500°K. At about 3000-3500°, the reduction of the carbide to the metal with formation of CO produces a substantial cooling effect with the equilibrium wall temperature over 1000° cooler than the free stream temperatures.

BeF_2

This system shows essentially a constant saturation number as was found also for tungsten with this gas[2]. Basically the BeF_2 is dissociating to BeF and F, the free fluorine then reacting with the condensed phase. The overall reaction is endothermic at low temperature (640° at 2500°) and exothermic at high temperature (1100° at 4500°). It should be mentioned that these results are based on the JANAF value of -88.34 kcal/mole for the standard heat of formation of BeF at 298°K;a less negative value which now appears probable[5] would presumably materially alter the results.

CO

Very little reaction takes place over the whole temperature range, as would be expected. Some cooling occurs at very high temperatures (53°K at 5000°K; 11°K at 4500°K) due to volatilization.

CO_2

The corrosion is essentially due to oxygen from dissociation of CO_2. At temperatures below 3500°K, Ta_2O_5/c is formed; at temperatures somewhat above 3500°K, Ta/c is formed. The latter reaction results in a larger saturation value than the former. The reaction becomes strongly exothermic at high temperature (-211° at 2500°, +255° at 3000° and 1497° at 4500°).

HCl

This gas reacts primarily (and exothermically) with TaC/c to form H_2, solid carbon, and gaseous tantalum chlorides. Saturation numbers decrease with temperature due to decreasing stability of the tantalum chlorides and increase in the fraction of chlorine that remains in the elemental form. The equilibrium wall temperature is some 100-400° greater than the free stream.

HF

This gas behaves chemically in a fashion similar to HCl. The heating effect is greater at low temperatures (nearly 1000°K) and less at high temperatures (about 100°K at 5000°).

H_2

Very little reaction occurs below about 3000°K, at which temperature the saturation reaction is slightly exothermic (23°K). The saturation numbers increase with temperature as more gaseous hydrocarbons and elemental metal are formed; the net heating effect decreases gradually until at 5000°K the net reaction is endothermic by 1.3°K.

H_2O

Up to 3000°K, Ta_2O_5 is the primary reaction product, and is formed nearly quantitatively. At higher temperatures elemental tantalum forms. The saturation numbers are high over the whole range indicating that H_2O is extremely corrosive to TaC. The reactions are exothermic in the lower temperature region and strongly endothermic where Ta_2O_5 is not stable and Ta/c forms.

LiF

No gas phase is computed below about 3500°K. Gaseous products include tantalum and carbon fluorides along with gaseous lithium. The overall reactions are very slightly endothermic (15°K-50°K) over the 3500-5000°K range.

N_2

TaC reacts quantitatively with N_2 to form TaN and carbon at low temperatures (see Section 5). At 3000° the reaction is exothermic, so that the adiabatic wall is some 400°K hotter than the free stream. The reaction is exothermic to about this same degree to 4500°K; at 5000°K the reaction is only 38°K exothermic due to increase in endothermic volatilization effects. CN is the primary gaseous reaction product.

2.2 RECALCULATION OF THE CORROSION OF TUNGSTEN BY BOF, CO AND CO_2

Since publication of the Third Quarterly Report[2], revised or new data sheets have been issued for the JANAF tables[3] on the WO_3/c, WO_3(g), W_3O_9(g) and W_4O_{12}(g) species. As substantial changes were involved, computations for cases where these oxides might be significant were repeated. (The tungsten-water case has again been held up pending anticipated receipt of new information on H_2WO_4(g)[4]. The HBO_2 case was not recomputed in view of the rather meaningless results obtained before[2], with no gas phase present at 1000 psia below about 4500°K.)

Results are given in Figures 7 and 8.

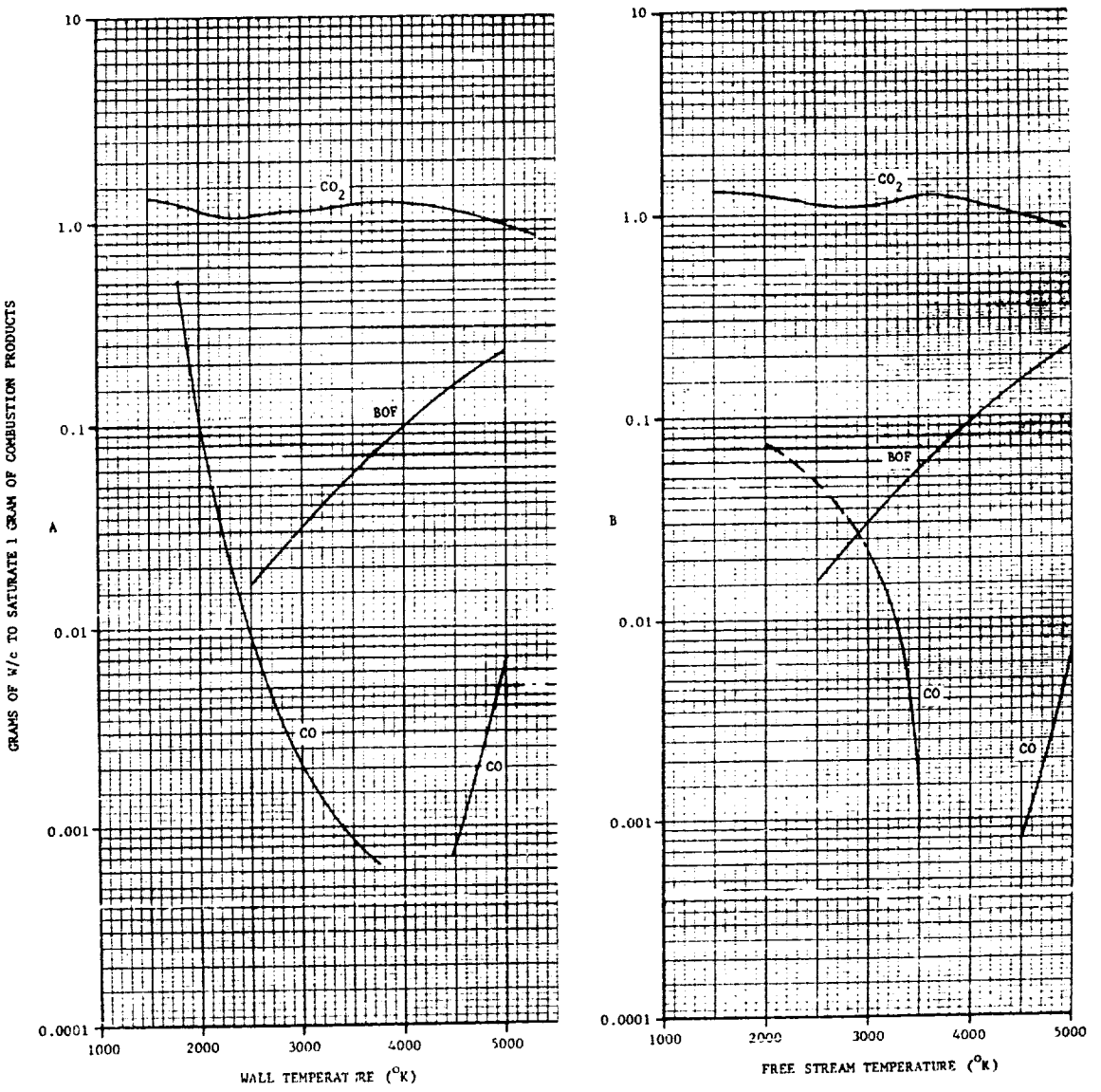

FIGURE 7. CHEMICAL CORROSION OF TUNGSTEN BY BOF, CO AND CO_2 AT 1000 PSIA (REVISED CALCULATIONS)

Ford Motor Company
AERONUTRONIC DIVISION

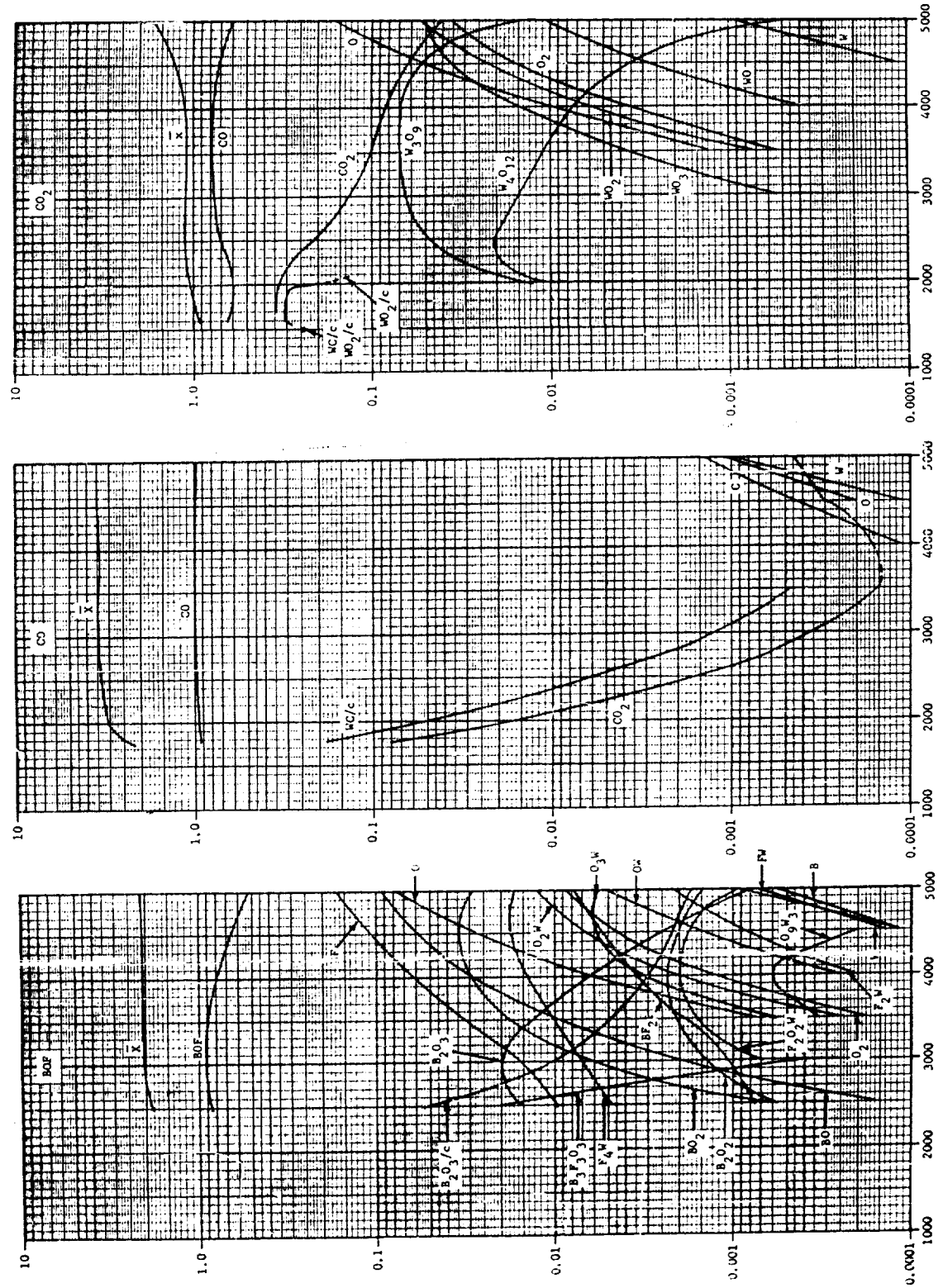

R00120

FIGURE 8. SPECIES PRESENT UNDER EQUILIBRIUM CONDITIONS AT 1000 PSIA FOR TUNGSTEN AND BOF, CO AND CO_2 (REVISED CALCULATIONS)

Comparison of the results with the new and old data can be made by examining Table II. The most striking effect is on the 3500°K point with CO_2; the revised data show a substantial (592°K) increase in adiabatic saturation temperature over free stream temperature whereas the older data showed a significant (205°) cooling effect. This is due to a reduction in the enthalpy of saturated system at a given temperature with the revised data, as shown by the "hsw" values given in Table II. "B" values are not greatly affected, inasmuch as the revised data show W_3O_9 concentrations which are roughly one-third of the WO_3 concentration computed earlier. This is shown in Table III.

Comments on the individual systems follow.

BOF-W

This system is all condensed at 1500 and 2000°K at 1000 psia (WOF_4/c and B_2O_3/c). B_2O_3/c disappears above 2000°K. The polymeric tungsten oxide vapor species are not particularly important. The reactivity increases with temperature.

CO-W

At 1500°K and 1000 psia this system is all condensed, forming WC/c and WO_2/c. A gas phase appears between 1500 and 2000°K and reactivity decreases to nearly zero at about 4000°K at which point it begins to increase due to simple volatilization of tungsten. These results are of course sensitive to the thermodynamic data used for WC/c, which are not well known. No gas phase tungsten oxide is significant.

CO_2-W

This system also forms WC/c and WO_2/c at 1500°K. WC/c disappears below 2000°K; WO_2/c disappears below 2500°K. The polymeric tungsten oxide species are primary contributors to the ablation. (WO_3(g) was indicated to be the primary contributor in the last Quarterly Report[2].)

TABLE II

COMPARISON OF RESULTS OF ABLATION COMPUTATIONS USING "OLD" AND REVISED JANAF THERMODYNAMIC DATA FOR TUNGSTEN OXIDES

1000 psia

Free Stream Temp., °K	Wall Temperature, °K		B Parameter	
	"Old"	Revised	"Old"	Revised
System W-BOF				
3000	2962	2969	.0307	.0292
3500	3412	3443	.0631	.0526
4000	3901	3947	.1275	.0943
4500	4459	4478	.2257	.1563
5000	5021	5004	.3098	.2234
System W-CO				
2000	2057	2057	.0773	.0773
3500	3501	3501	.0009	.0009
4000	4000	4000	.00004	.00004
4500	4498	4498	.0008	.0008
5000	4981	4981	.0065	.0065
System W-CO_2				
3000	2843	2804	1.008	1.148
3500	3295	4092	1.153	1.240
4000	4611	4659	1.227	1.141
4500	5232	4984	1.241	0.984
5000	5624	5312	0.911	0.814

TABLE III

COMPARISON OF EQUILIBRIUM GAS MOLE FRACTIONS
CO_2 plus W, 1000 psia

"Old" and "Revised" as in Table II

	3000°		3500°		4000°	
Species	Old	Revised	Old	Revised	Old	Revised
CO	.7222	.7781	.6704	.8058	.6947	.8032
CO_2	.1839	.1401	.1051	.1035	.0644	.0829
O	.0001	--	.0017	.0014	.0099	.01104
WO	--	--	--	--	.0004	.0004
O_2	.0001	.0001	.0009	.0006	.0031	.0038
WO_2	.0001	--	.0011	.0008	.0045	.0056
WO_3	.0912	.0005	.2203	.0037	.2231	.0145
W_3O_9	.00238	.0656	.0004	.0730	--	.0709
W_4O_{12}	--	.0155	--	.0111	--	.0076
WO_3/c*	.169					
$\bar{x}$**	1.190	1.137	1.334	1.120	1.326	1.143
hsw***	-40.16	-41.52	-15.02	-30.77	-4.15	-18.67

* Moles/100 grams of system on an excess tungsten-free basis

** Moles gas on same basis

*** In kcal/100 grams on same basis $/\bar{}\Sigma x_i(\Delta H^o_{f298} + H^+_{298})_i\bar{}/$

2.3 REFRACTORY OXIDES FOR USE IN OXYGEN-CONTAINING ATMOSPHERES

Equilibrium calculations have been made during the course of this work on a variety of refractory materials, including graphite and tungsten as well as certain carbides and borides. All of these materials have been found to be subject to fairly severe attack in oxygen-containing atmospheres (such as CO_2 and H_2O), a fact which leads immediately to consideration of refractory oxides as materials for such applications. Unfortunately, the oxides generally melt at much lower temperatures than do the other materials of interest so that they are not obviously attractive for high temperature application. This is shown by the figures in the following list:

Compound	Melting Point, $^{\circ}K$
TaC	4100
HfC	4160
W	3650
C	$\sim$4100 (sublimes at 1 atm)
HfN	3580
HfB_2	3520
ThO_2	3323
HfO_2	3170
MgO	3073
BeO	2823

The highest melting oxide is ThO_2, which melts at a temperature of $3323^{\circ}K$ or $5521^{\circ}F$, a temperature far below that expected with many advanced propellant systems of interest. There did, however, appear to be some possibility that these materials would be self-cooled by their own vaporization processes, which if appreciable, could make their usefulness somewhat greater than would be immediately apparent. A brief study was thus made of the cooling effect involved with CO_2 as a nominal gas using the refractory oxides MgO, HfO_2 and ThO_2. MgO was studied because it is, in

the region of interest, the most volatile of the high melting oxides; HfO_2 because it is the last volatile[6], and of course ThO_2 because it is the highest melting oxide.

The procedure used was the same as that employed in other cases studied, except that attention was devoted to the cooling effect during adiabatic saturation as a function of pressure. Thermodynamic data for the MgO system were based on the JANAF tables to the melting point ($3073^{\circ}K$)[7] at which a heat of fusion of 18.5 kcal/mole was assigned and above which a constant heat capacity of 14.0 cal/mole-$^{\circ}K$ was used. The data for HfO_2 and its compounds was that reported previously in this work[2]. These two cases were computed using the Aeronutronic machine ablation program[1,2]; the ThO_2 case was considered only by relatively crude hand computation methods inasmuch as the thermodynamic data available for ThO_2[8] have not been worked up into a form suitable for inclusion in our machine program.

Equilibrium computation results for MgO and HfO_2 are shown for the three cases studied in Figure 9 through 13. Examination of the "A" and "B" plots reveals that relatively little cooling effect can be anticipated in the vicinity of the melting point, and that where cooling is substantial, saturation values are high. The cooling effect in the CO_2 case is made more clearly evident in Figure 13; a similar plot for the HfO_2 case would show substantially less deviation from the 45° line. (At $3500^{\circ}K$ and 10 psia, the cooling effect with HfO_2 is only $5^{\circ}K$.)

The self-cooling effect due to volatilization of the oxides is summarized along with "B" values, at the melting point, for the three cases studied in Table IV. The cooling effect, which is shown in the final column, denotes the difference between the free stream stagnation temperature and the wall temperature at the melting point (under, of course, the assumptions used in this work). Obviously, the cooling effect is greater at lower pressure but in no case is it very great. With MgO, for example, the free stream stagnation temperature can be only approximately 270° above the

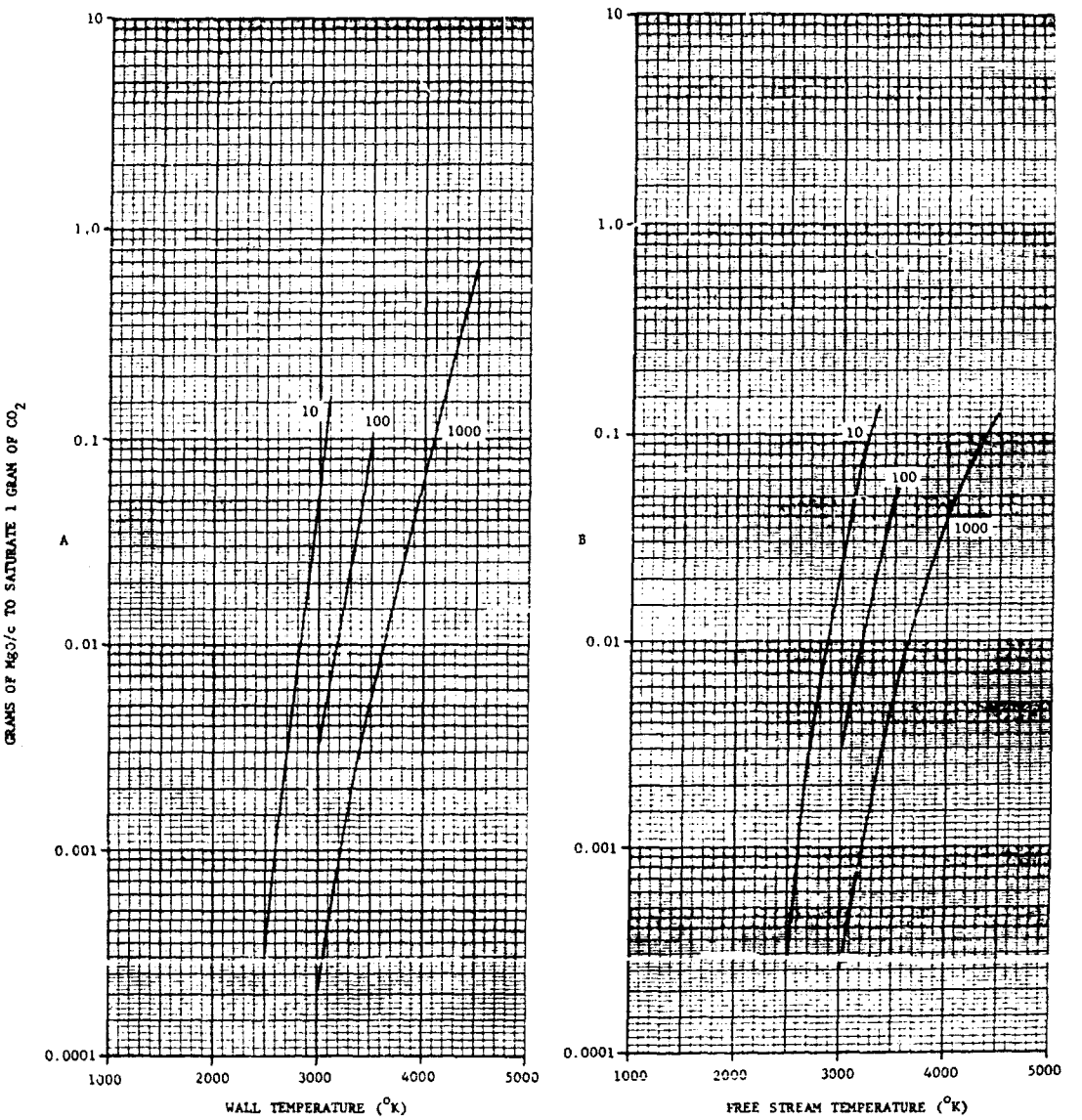

FIGURE 9. CHEMICAL CORROSION OF MgO BY CO_2 AT THREE PRESSURES

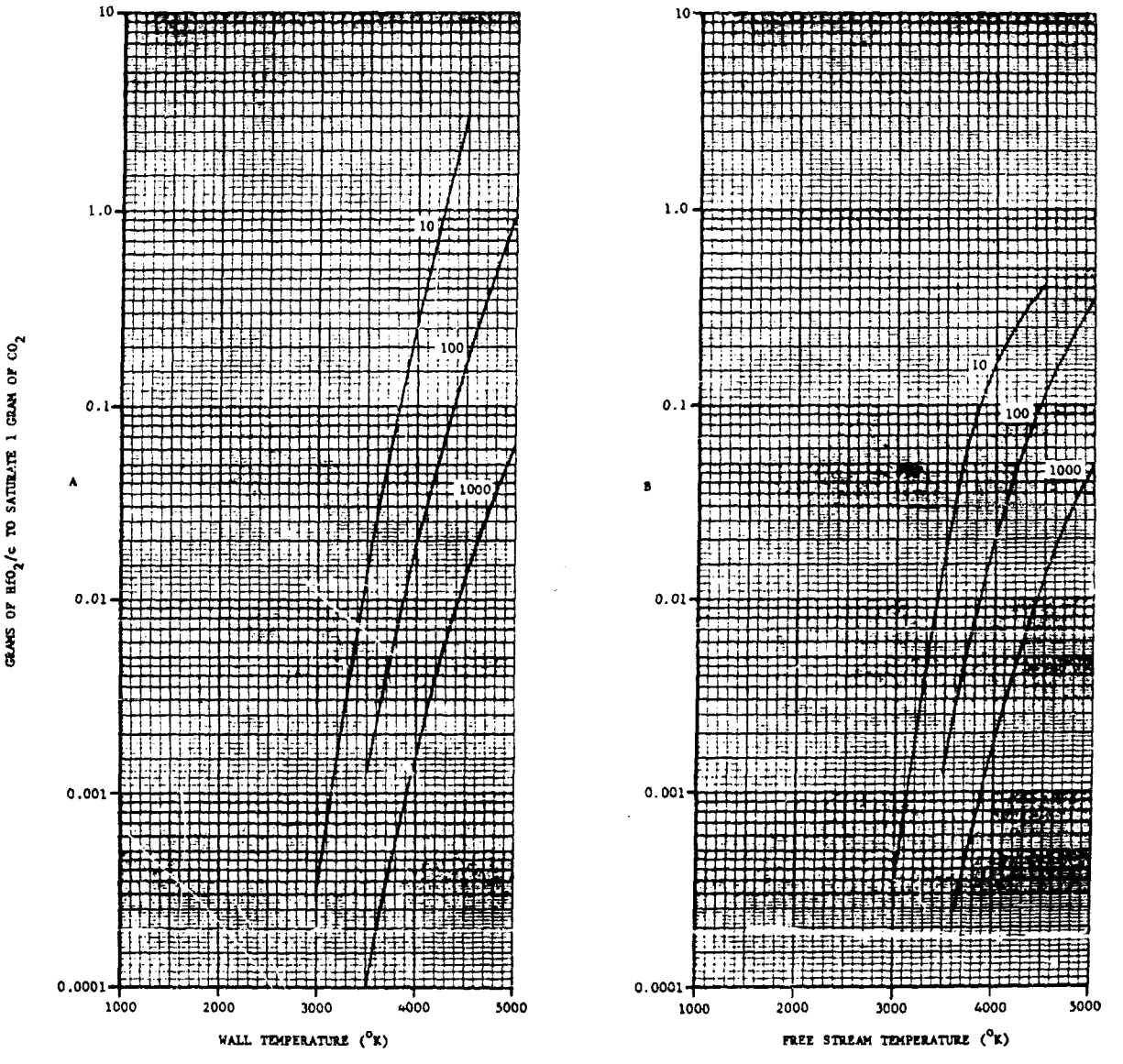

R00122

FIGURE 10. CHEMICAL CORROSION OF HfO_2 BY CO_2 AT THREE PRESSURES

Ford Motor Company
AERONUTRONIC DIVISION

R00123

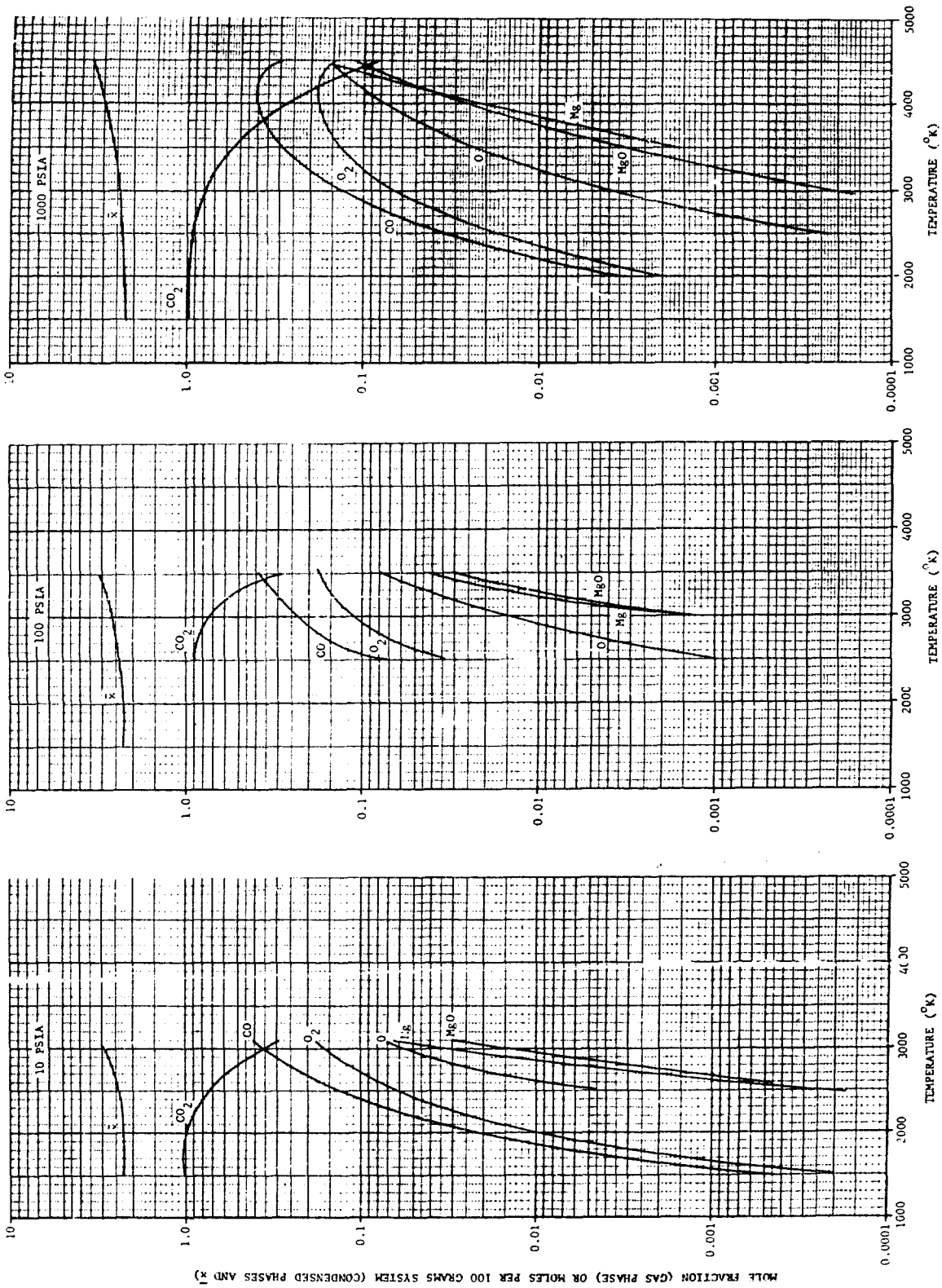

FIGURE 11. SPECIES PRESENT UNDER EQUILIBRIUM CONDITIONS AT THREE PRESSURES FOR CO_2 AND MgO

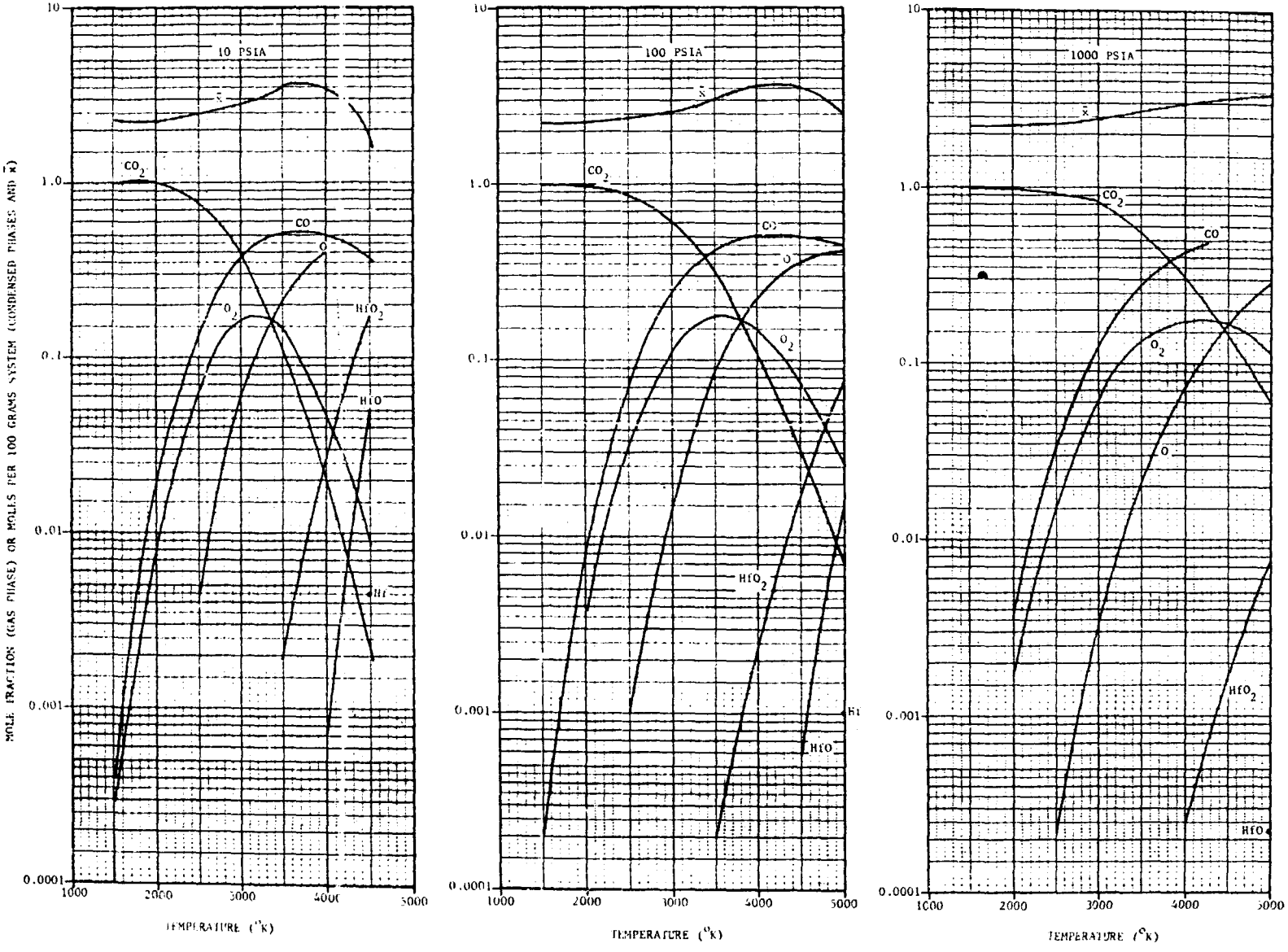

R00124

FIGURE 12. SPECIES PRESENT UNDER EQUILIBRIUM CONDITIONS AT THREE PRESSURES FOR CO_2 AND HfO_2

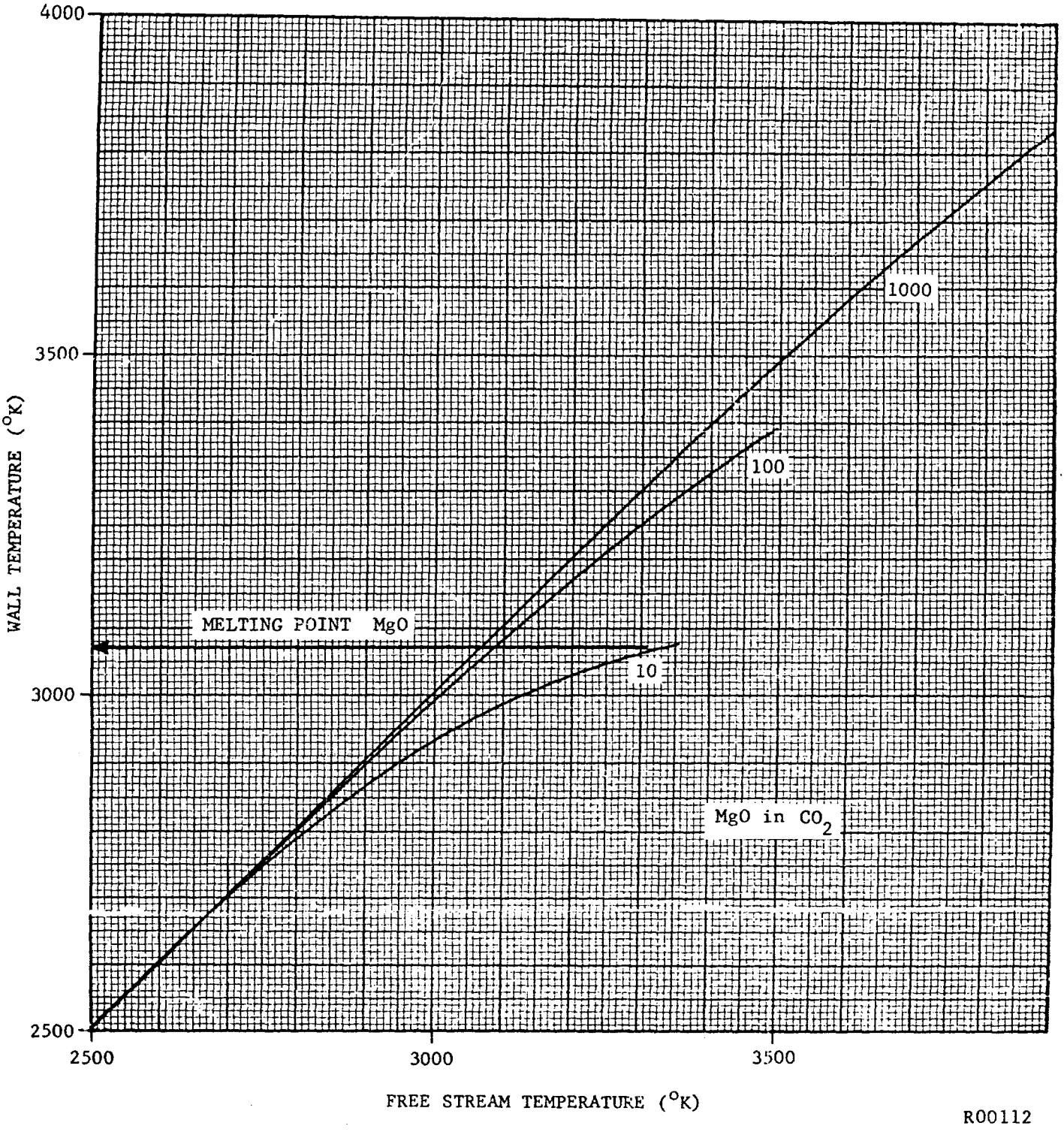

FIGURE 13. ADIABATIC WALL TEMPERATURE VS. FREE STREAM TEMPERATURE FOR MgO IN CO_2 AT THREE PRESSURES

TABLE IV

WALL COOLING EFFECTS WITH MgO, HfO_2 AND ThO_2 AT THEIR MELTING POINTS IN A CO_2 ATMOSPHERE AT VARIOUS PRESSURES

Oxide	Melting Point, °K	Pressure, psia	"B" grams/grams	Cooling Effect, °K
MgO	3073	1000	4.1×10^{-4}	~3
		100	6.1×10^{-3}	~18
		10	1.4×10^{-1}	~270
HfO_2	3170	1000	~0	~0
		100	9.0×10^{-4}	~1
		10	1.3×10^{-3}	~3
ThO_2	3323	1000	$\sim 2 \times 10^{-4}$	< 1
		100	$\sim 3 \times 10^{-3}$	~ 5
		10	$\sim 4 \times 10^{-2}$	~60

3073°K melting point of MgO or 3340°K, evan at 10 psia, before melting would be expected. With ThO_2 the maximum free stream temperature could be only about 3380°K even at 10 psia before melting would occur; the saturation parameter and thus the regression rate would be smaller than with MgO. With HfO_2, as expected, the cooling effect is very slight. In no case is the cooling effect of any real significance at pressures of interest in most rocket combustion systems.

Based on the foregoing limited analysis, the oxides do not appear attractive for high temperature oxygen-containing propellant systems. This of course does not preclude their consideration for all applications.

2.4 STABILITY OF CARBIDES IN NITROGEN

As refractory metal carbides are among the highest melting materials known, they are of considerable interest as possible nozzle materials and have been under investigation in this program in terms of their chemical stability. These studies have been limited in the case of the carbides reacting with nitrogen in that below certain temperatures at given pressures nitrogen reacts quantitatively with these carbides to form a condensed system consisting of metal nitrides and carbon; the program gives relatively little worthwhile information under these conditions. The nitrides are, however, lower melting than the corresponding carbides, as shown in the following tabulation:

Carbide	Melting Point, °K	Nitride	Melting Point, °K
HfC	4160	HfN	3580
TaC	4100	TaN	3363
ZrC	3765	ZrN	3225
TiC	3410	TiN	3200

so that it becomes important to know under what conditions carbides are thermodynamically unstable in nitrogen. (Tungsten apparently forms no nitrides of interest[2].) A brief study carried out in this direction ensues.

The pressure of nitrogen in equilibrium with the three condensed phases, C, nitride, and carbide, was computed from previously reported[1,2] and JANAF thermodynamic data, based on the equation:

$$MeC/c + \tfrac{1}{2}N_2(g) \rightleftharpoons C/c + MeN/c \qquad (1)$$

where

Me = Ti, Zr, Hf or Ta.

At the nitrogen pressures and temperatures involved in the study, the extent of the nitrogen dissociation reaction

$$N_2(g) \rightleftharpoons 2N(g) \qquad (2)$$

and the carbide and nitride dissociation reactions

$$MeN/c \rightleftharpoons Me(g) + \tfrac{1}{2}N_2(g) \qquad (3)$$

and

$$MeC/c \rightleftharpoons Me(g) + C/c \qquad (4)$$

was found to be negligible so that it was necessary to consider only the primary reaction (Reaction 1). Hand computational methods were thus used.

The N_2 pressure results are plotted against reciprocal temperatures in Figure 14. It is evident from the plot that at a given temperature TaC requires the greatest nitrogen pressure to convert it to the carbide and HfC requires the least. The relative stabilities of the carbides in nitrogen can thus be said to decrease in the order TaC, TiC, ZrC and HfC. Even HfC, the least stable of these, however, requires a N_2 pressure of greater than 1000 psia at 2780°K to convert the carbide to the lower melting nitride; at higher temperatures (nearer the melting point) a pressure greater than 1000 psia would be required. If nitride formation is to occur in a carbide nozzle under neutral conditions in a nitrogen atmosphere, it would form thermodynamically only during the transient heat up period and would not be of concern at the higher temperature conditions normally of interest. These

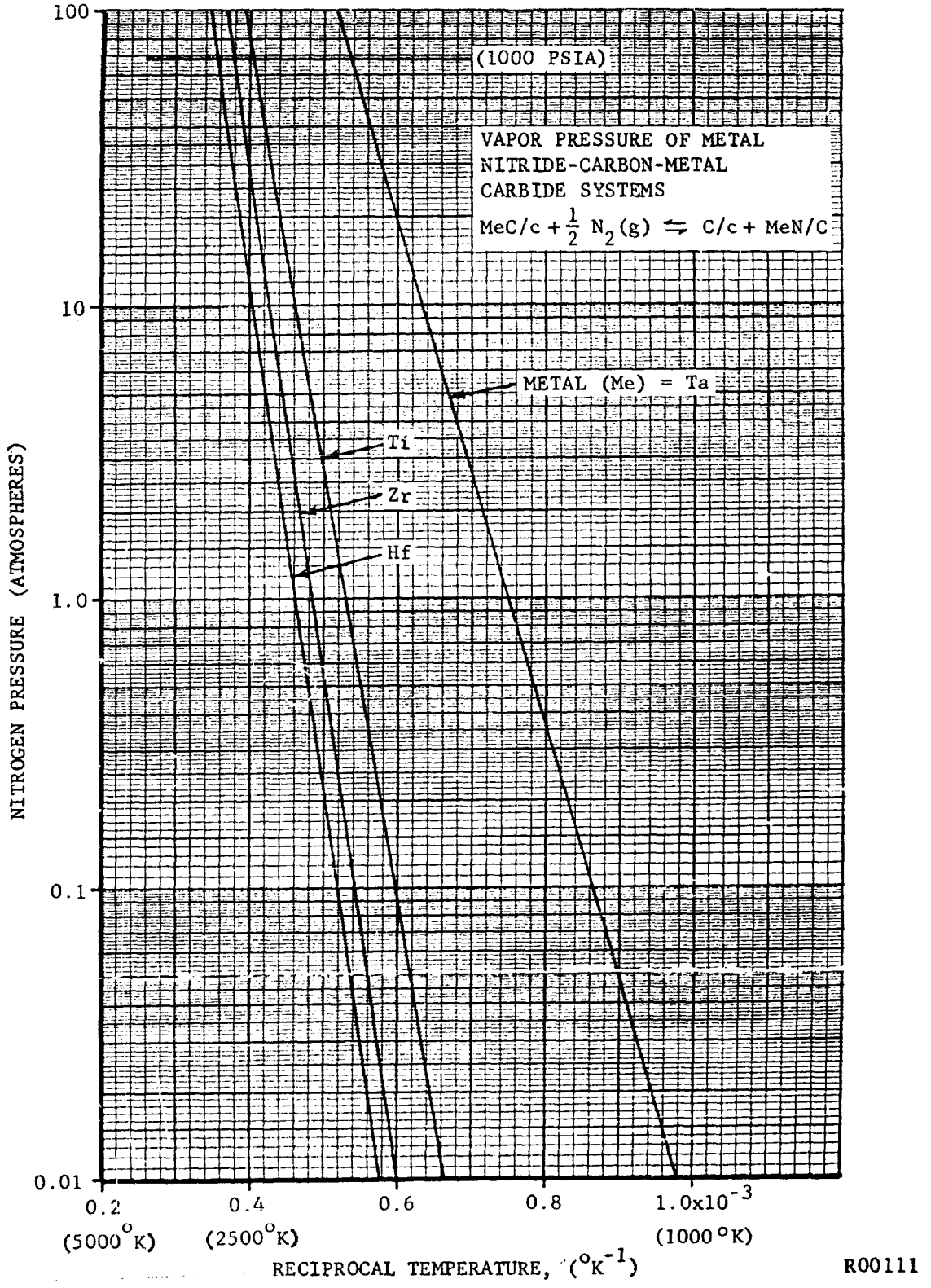

FIGURE 14. VAPOR PRESSURES OF REFRACTORY NITRIDES IN EQUILIBRIUM WITH BOTH CARBON AND THE CARBIDE

computations are of course valid only for the unique conditions considered. Should an additional reactant be present so that solid carbon is not present, nitrides may form with specified nitrogen pressures at considerably higher temperature conditions.

For the sake of completeness, the computations given in previous reports for the various carbide-nitrogen cases can be extended into the all-condensed regions in terms of the "A" saturation parameter, using the information presented in Figure 14*. These computations were made for 1000 psia nitrogen pressure so that at temperatures below the corresponding temperature in Figure 14 the carbide would be quantitatively converted to nitride and the "A" value would be simply:

$$A = \frac{\text{grams metal carbide}}{\text{gram nitrogen}} = \frac{\text{molecular weight of the carbide}}{14.007}$$

In the case of TaC for example at 1000 psia below 1850°K, the A value would be simply

$$A = \frac{192.96}{14.007} = 13.8$$

At temperatures above 1850°K at 1000 psia, the A value would be zero until temperatures at which CN gaseous species become significant. The corresponding temperature at 1000 psia for the other systems would be about 2440°K for TiC, 2630°K for ZrC, and 2780°K for HfC. Figure 14 is useful for other systems and other pressures in a similar way. For example, at 1500°K the equilibrium nitrogen pressure with TaC is 5.5 atmospheres or 81 psia. Below this pressure there is no tendency for reaction to occur; above this pressure the A value would be 13.8.

Values for the adiabatic saturation parameters can not be readily determined using this simple approach.

---

* The equilibrium composition plots in these cases actually start at temperatures considerably above the all-condensed region, inasmuch as finite quantities ($>10^{-6}$ mole/100 grams) of vapor species formed from the reactant solid must normally be present in the Aeronutronic computer program for computation to proceed. Thus where the gas is 100% N_2 and the solid is simply TaC the ablation program rejects the problem and goes to a higher temperature. In the TaC case at 1000 psia, the first machine results are at 3000°K where CN(g) is present at a mole number of 5×10^{-6}; Figure 14 however shows that conversion to all condensed occurs only below 1850°K.

SECTION 3

PREDICTION OF ISOTHERMAL SATURATION NUMBERS FOR MIXTURES FROM DATA ON "PURE" COMPONENTS, WITH ALLOWANCE FOR TOTAL PRESSURE EFFECTS

3.1 INTRODUCTION

In order to extend the utility of isothermal and adiabatic saturation numbers being determinedunder this contract for nozzle materials corroded by "pure" combustion system components (CO, H_2O, BOF, etc.), a tentative approach has been developed for predicting from these numbers the corrosivities of complex mixtures of combustion products and at total pressures other than those reported. Initially, the method has been confined to the estimation of isothermal saturation numbers "A" for such mixtures. Whereas the prediction of adiabatic saturation numbers "B" for mixtures based on data for the pure components appears next to impossible, such numbers for complex systems might be correlated empirically, knowing the general relationship between "A" and "B" for the individual components. Accordingly, corrosion rates might be estimated for actual propulsion applications, assuming the adiabatic saturation model.

The method thus developed is not intended to replace the rigorous calculation of saturation numbers, using the ablation equilibrium computer program. Rather, it is designed to permit rapid estimation of "A" values for cases where a computer or suitable program is not available, or in which rigorous computation would require excessive use of machine time.

The basis of the approach first will be outlined, including the preliminary "additivity" assumption, and the more elaborate model subsequently developed. Mathematical treatments then will be given for four typical cases, and possible extensions to other situations will be indicated. Finally, two examples will be presented, showing actual comparisons between predicted and rigorously computed isothermal saturation numbers.

3.2 THEORETICAL BASIS

A simple assumption which might be used to estimate isothermal saturation numbers "A" for complex systems is the rule of "additivity", in which the overall "A" would be taken as a linear, weighted average of the "A's" of each of the individual combustion species. In applying this approach, the "A" for each component would be taken at the total system pressure, rather than at its own partial pressure, since otherwise, "A" values of infinity might be determined for some trace species. Even with this technique, an "A" value for a certain species may be undefined, if a question exists as to whether the species yields a gaseous phase in equilibrium with the ablator at the specified temperature and pressure.

As will be shown, the "additivity" model by itself yields correct predictions of isothermal saturation numbers only for a very limited number of systems. Two obvious factors tending to invalidate this assumption are: (1) partial pressure effects on equilibria involving a change in gaseous moles, and (2) chemical interaction between two corrodant species. The method herein developed is concerned primarily with applying "corrections" based upon factor (1) for the case of dilution of the attacking species by an essentially inert carrier gas. By some modification, the approach can be expanded to include dilution by an independently corrosive agent, or, under factor (2), even dilution by a second species entering into the same equilibrium reaction. The only situation not amenable to direct analysis is that in which a new ablation species appears upon going to the complex system.

3.3 A CATALOG OF ABLATION REACTIONS

In order to characterize ablation reactions for possible pressure effects, four main groupings were defined, as shown in Table V, according to whether the net mole change was zero, positive, negative, or independent of the gaseous species. Various ablation reactions, involing corrosion of C/c, TiC/c, ZrC/c, ZrB_2/c and W/c nozzle materials have been classified according to this scheme; the results are presented in Table VI. As an approximation, any reaction involving a mole change of less than 50 percent (2→3, or 3→2), has been considered as having zero change in gaseous moles.

TABLE V

CLASSIFICATION OF ABLATION REACTIONS

Case	Description	Type	Gas-Phase Mole Reaction
I	No change in gaseous moles	I	n→n
II	Increase in gaseous moles	II	1→2
		II'	2→3
		II''	1→3
		II'''	1→4 and higher
		II(4)	0→n
III	Decrease in gaseous moles	III	2→1
		III'	3→2
		III''	n→0
IV	Inert gas feed; simple decomposition or vaporization of ablator	IV	0→n

TABLE VI

A CATALOG OF ABLATION REACTIONS

(Pressure = 1000 psia)

Corrodant	Principal Reaction	Type	Temp., ^{o}K	A	B
	Ablator: C/c				
H_2O	$C/c + H_2O \longrightarrow CO + H_2$	II	2000	0.66	0.44
H_2O	$C/c + H_2O \longrightarrow CO + H_2$	II	3000	0.77	0.63
H_2O	$3C/c + H_2O \longrightarrow CO + C_2H_2$	II	4000	1.50	0.86
H_2	$C/c + 2H_2 \longrightarrow CH_4$	III	2000	0.15	0.14
H_2	$2C/c + H_2 \longrightarrow C_2H_2$	I	3000	0.84	0.18
H_2	$2C/c + H_2 \longrightarrow C_2H_2$	I	4000	6.6	1.20
CO_2	$C/c + CO_2 \longrightarrow 2CO$	II	2000	0.26	0.082
CO_2	$C/c + CO_2 \longrightarrow 2CO$	II	3000	0.27	0.22
CO_2	$C/c + CO_2 \longrightarrow 2CO$	II	4000	0.28	0.31
HF	$2C/c + 2HF \longrightarrow C_2F_2 + H_2$	I	2000	0.0008	0.0008
HF	$2C/c + 2HF \longrightarrow C_2F_2 + H_2$	I	3000	0.018	0.013
HF	$2C/c + 2HF \longrightarrow C_2F_2 + H_2$	I	4000	0.24	0.076
N_2	$2C/c + N_2 \longrightarrow 2CN$	II	3000	0.0027	0.0020
N_2	$2C/c + N_2 \longrightarrow 2CN$	II	4000	0.11	0.020

TABLE VI: A CATALOG OF ABLATION REACTIONS (Pressure = 1000 psia) (page 2)

Corrodant	Principal Reaction	Type	Temp., °K	A	B
	Ablator: C/c (continued)				
HCl	$2C/c + 2HCl \rightarrow C_2H_2 + 2Cl$	II'	3000	0.0022	0.0018
HCl	$2C/c + HCl \rightarrow C_2H + Cl$	II	4000	0.095	0.038
CO	$3C/c \rightarrow C_3$	IV	4000	0.0072	0.0044
Al_2O_3/c	$3C/c + Al_2O_3/c \rightarrow 2Al + 3CO$	II(4)	3000	0.51	---
Al_2O_3/c	$3C/c + Al_2O_3/c \rightarrow 2Al + 3CO$	II(4)	4000	0.36	0.056
HBO_2	$2C/c + 2HBO_2 \rightarrow H_2 + 2CO + B_2O_2$	II	2000	0.37	0.13
HBO_2	$2C/c + 2HBO_2 \rightarrow H_2 + 2CO + B_2O_2$	II	3000	0.60	0.26
HBO_2	$4C/c + HBO_2 \rightarrow C_2H + 2CO + B/c$	II''	4000	0.74	0.43
BOF	$C/c + BOF \rightarrow CO + BF$	II	2000	0.013	0.013
BOF	$C/c + BOF \rightarrow CO + BF$	II	3000	0.25	0.094
BOF	$C/c + BOF \rightarrow CO + BF$	II	4000	0.27	0.15
BF_2	$C/c + 12BF_2 \rightarrow 8BF_3 + B_4C/c$	III'	2000	0.012	0.0084
BF_2	----------	---	3000	~ 0	~ 0
BF_2	$2C/c + 2BF_2 \rightarrow C_2F_2 + 2BF$	II'	4000	0.023	0.010
BeF_2	$2C/c + 2BeF_2 \rightarrow C_2F_2 + 2BeF$	II'	2000	0.004	0.022
BeF_2	$2C/c + 2BeF_2 \rightarrow C_2F_2 + 2BeF$	II'	3000	0.14	0.087
BeF_2	$2C/c + 2BeF_2 \rightarrow C_2F_2 + 2BeF$	II'	4000	0.23	0.25

TABLE VI: A CATALOG OF ABLATION REACTIONS (Pressure = 1000 psia) (page 3)

Corrodant	Principal Reaction	Type	Temp., °K	A	B
	Ablator: C/c (continued)				
BeO/c	$3C/c + BeO/c \rightarrow Be_2C/c + CO$	II[(4)]	3000	0.0001	0.0001
BeO/c	$C/c + BeO/c \rightarrow Be + CO$	II[(4)]	4000	0.73	0.67
BF_3	$2C/c + 2BF_3 \rightarrow C_2F_2 + 2BF_2$	II'	3000	0.0033	0.0026
BF_3	$2C/c + 2BF_3 \rightarrow C_2F_2 + 2BF_2$	II'	4000	0.088	0.038
AlF_3	$2C/c + 2AlF_3 \rightarrow C_2F_2 + 2AlF_2$	II'	3000	0.0024	0.0021
AlF_3	$2C/c + 2AlF_3 \rightarrow C_2F_2 + 2AlF_2$	II'	4000	0.045	0.025
LiF	$2C/c + 2LiF \rightarrow C_2F_2 + 2Li$	II'	4000	0.019	0.013
	Ablator: TiC/c				
H_2O	$2TiC/c + 5H_2O \rightarrow Ti_2O_3/c + 2CO + 5H_2$	I	2000	1.28	1.29
H_2O	$TiC/c + 2H_2O \rightarrow TiO/c + CO + 2H_2$	II'	3000	1.67	1.39
H_2O	$TiC/c + H_2O \rightarrow Ti + CO + H_2$	II''	4000	2.86	2.05
H_2	$2TiC/c + H_2 \rightarrow 2Ti/c + C_2H_2$	I	3000	0.0068	0.0062
H_2	$2TiC/c + H_2 \rightarrow 2Ti + C_2H_2$	II''	4000	0.70	0.35
CO_2	$2TiC/c + 5CO_2 \rightarrow Ti_2O_3/c + 7CO$	I	2000	---	---
CO_2	$2TiC/c + 5CO_2 \rightarrow Ti_2O_3/c + 7CO$	I	3000	0.55	0.58
CO_2	$TiC/c + 2CO_2 \rightarrow TiO/c + 3CO$	II'	4000	0.75	0.81

TABLE VI: A CATALOG OF ABLATION REACTIONS (Pressure = 1000 psia) (page 4)

Corrodant	Principal Reaction	Type	Temp., °K	A	B
	Ablator: TiC/c (continued)				
HF	$TiC/c + 4HF \rightarrow C/c + TiF_4 + 2H_2$	I	2000	0.84	0.89
HF	$TiC/c + 4HF \rightarrow C/c + TiF_4 + 2H_2$	I	3000	2.2	1.13
HF	$2TiC/c + 2HF \rightarrow C_2H_2 + 2TiF$	II'	4000	2.9	1.79
N_2	$2TiC/c + N_2 \rightarrow 2TiN/c + 2C/c$	III''	2000	---	---
N_2	$2TiC/c + N_2 \rightarrow 2Ti + 2CN$	II'''	3000	0.0024	0.0021
N_2	$2TiC/c + N_2 \rightarrow 2Ti + 2CN$	II'''	4000	0.042	0.020
HCl	$TiC/c + 4HCl \rightarrow TiCl_4 + 2H_2 + C/c$	I	2000	0.33	0.28
HCl	$2TiC/c + 6HCl \rightarrow 2TiCl_3 + 3H_2 + 2C/c$	I	3000	0.27	0.28
HCl	$2TiC/c + 2HCl \rightarrow 2TiCl + C_2H_2$	II'	4000	0.49	0.41
CO	$2TiC/c + 3CO \rightarrow Ti_2O_3/c + 5C/c$	III''	2000	---	---
CO	$2TiC/c + 3CO \rightarrow Ti_2O_3/c + 5C/c$	III''	3000	---	---
CO	$TiC/c \rightarrow Ti + C$	IV	4000	0.0084	0.0056
	Ablator: ZrC/c				
H_2O	$ZrC/c + 2H_2O \rightarrow ZrO_2/c + C/c + 2H_2$	I	2000	1.3	2.0
H_2O	$ZrC/c + 3H_2O \rightarrow ZrO_2/c + CO + 3H_2$	I	3000	2.4	2.0
H_2O	$ZrC/c + H_2O \rightarrow Zr/c + CO + H_2$	II	4000	5.4	3.7

TABLE VI: A CATALOG OF ABLATION REACTIONS (Pressure = 1000 psia) (page 5)

Corrodant	Principal Reaction	Type	Temp., °K	A	B
	Ablator: ZrC/c (continued)				
H_2	$2ZrC/c + H_2 \rightarrow 2Zr/c + C_2H_2$	I	3000	0.0008	0.0008
H_2	$2ZrC/c + H_2 \rightarrow 2Zr/c + C_2H_2$	I	4000	0.041	0.051
CO_2	$ZrC/c + 3CO_2 \rightarrow ZrO_2/c + 4CO$	I	3000	0.77	0.81
CO_2	$ZrC/c + 3CO_2 \rightarrow ZrO_2/c + 4CO$	I	4000	0.82	2.1
HF	$ZrC/c + 4HF \rightarrow C/c + ZrF_4 + 2H_2$	I	2000	1.3	2.4
HF	$ZrC/c + 2HF \rightarrow C/c + ZrF_2/c + H_2$	III	3000	2.4	2.5
HF	$2ZrC/c + 2HF \rightarrow C_2H_2 + ZrF_2/c$	III	4000	2.5	2.5
N_2	$2ZrC/c + N_2 \rightarrow 2ZrN/c + 2C/c$	III''	2000	---	---
N_2	$2ZrC/c + N_2 \rightarrow 2Zr/c + 2CN$	II	3000	0.0059	0.0059
N_2	$2ZrC/c + N_2 \rightarrow 2Zr/c + 2CN$	II	4000	0.074	0.065
HCl	$2ZrC/c + 6HCl \rightarrow 2C/c + 2ZrCl3 + 3H_2$	I	2000	0.94	0.94
HCl	$2ZrC/c + 6HCl \rightarrow 2C/c + 2ZrCl3 + 3H_2$	I	3000	0.95	1.03
HCl	$2ZrC/c + 2HCl \rightarrow 2ZrCl + C_2H_2$	II'	4000	1.32	1.32
CO	$ZrC/c + CO \rightarrow C + ZrO$	II	4000	0.0007	0.0007
	Ablator: ZrB_2/c				
H_2O	$ZrB_2/c + 5H_2O \rightarrow ZrO_2/c + B_2O_3/c + 5H_2$	I	2000	1.29	1.43
H_2O	$ZrB_2/c + 4H_2O \rightarrow ZrO_2/c + 2BOH + 3H_2$	I	3000	1.48	1.48
H_2O	$ZrB_2/c + 4H_2O \rightarrow ZrO_2/c + 2BOH + 3H_2$	I	4000	1.57	1.61

TABLE VI: A CATALOG OF ABLATION REACTIONS (Pressure = 1000 psia) (page 6)

Corrodant	Principal Reaction	Type	Temp., ^{o}K	A	B
	Ablator: ZrB_2/c (continued)				
H_2	$ZrB_2/c \rightarrow Zr/c + 2B$	IV	3000	0.0006	0.0006
H_2	$ZrB_2/c \rightarrow Zr + 2B$	IV	4000	0.053	0.051
CO_2	$ZrB_2/c + 5CO_2 \rightarrow ZrO_2/c + B_2O_3/c + 5CO$	I	2000	1.1	---
CO_2	$ZrB_2/c + 4CO_2 \rightarrow ZrO_2/c + B_2O_2 + 4CO$	I	3000	0.59	0.62
CO_2	$ZrB_2/c + 4CO_2 \rightarrow ZrO_2/c + 2BO + 4CO$	II'	4000	0.62	0.73
HF	$ZrB_2/c + 10HF \rightarrow ZrF_4 + 2BF_3 + 5H_2$	I	2000	0.57	0.91
HF	$ZrB_2/c + 4HF \rightarrow ZrF_2/c + 2BF + 2H_2$	I	3000	1.25	1.08
HF	$ZrB_2/c + 4HF \rightarrow ZrF_2/c + 2BF + 2H_2$	I	4000	1.39	1.30
N_2	$2ZrB_2/c + 3N_2 \rightarrow 2ZrN/c + 4BN/c$	III''	2000	2.7	---
N_2	$2ZrB_2/c + 3N_2 \rightarrow 2ZrN/c + 4BN/c$	III''	3000	---	---
N_2	$ZrB_2/c \rightarrow Zr + 2B$	IV	4000	0.0021	0.0021
HCl	$2ZrB_2/c + 18\ HCl \rightarrow 2ZrCl_3 + 4BCl_3 + 9H_2$	I	2000	0.27	0.35
HCl	$2ZrB_2/c + 18\ HCl \rightarrow 2ZrCl_3 + 4BCl_3 + 9H_2$	I	3000	0.42	0.43
HCl	$2ZrB_2/c + 10\ HCl \rightarrow 2ZrCl_3 + 4BCl + 5H_2$	I	4000	0.43	0.44
CO	$ZrB_2/c \rightarrow Zr/c + 2B$	IV	3000	0.00054	0.00055
CO	$ZrB_2/c \rightarrow Zr + 2B$	IV	4000	0.011	0.010

TABLE VI: A CATALOG OF ABLATION REACTIONS (Pressure = 1000 psia) (page 7)

Corrodant	Principal Reaction	Type	Temp., ^{o}K	A	B
	Ablator: W/c				
AlF_3	$W/c + 4AlF_3 \rightarrow WF_4 + 4AlF_2$	I	2000	0.0045	0.0039
AlF_3	$W/c + 4AlF_3 \rightarrow WF_4 + 4AlF_2$	I	3000	0.165	0.079
AlF_3	$W/c + 2AlF_3 \rightarrow WF_4 + 2AlF$	II'	4000	0.59	0.33
BF_2	$W/c + 3BF_2 \rightarrow WB/c + 2BF_3$	III'	2000	1.15	0.64
BF_2	$W/c + 4BF_2 \rightarrow WF_4 + 4BF$	I	3000	0.045	0.026
BF_2	$W/c + 4BF_2 \rightarrow WF_4 + 4BF$	I	4000	0.57	0.30
BF_3	$W/c + 2BF_3 \rightarrow WF_4 + 2BF$	II'	2000	0.0069	0.0066
BF_3	$W/c + 2BF_3 \rightarrow WF_4 + 2BF$	II'	3000	0.36	0.128
BF_3	$W/c + 2BF_3 \rightarrow WF_4 + 2BF$	II'	4000	1.02	0.53
BOF	$W/c + 6BOF \rightarrow WF_4 + 2B_2O_3 + 2BF$	I	3000	0.032	0.031
BOF	$3W/c + 9BOF \rightarrow 3W_3O_9 + 9BF$	I	4000	0.136	0.121
HBO_2	----------	---	---	---	---
BeF_2	$W/c + 4BeF_2 \rightarrow WF_4 + 4BeF$	I	2000	0.88	---
BeF_2	$W/c + 4BeF_2 \rightarrow WF_4 + 4BeF$	I	3000	0.94	0.92
BeF_2	$W/c + 4BeF_2 \rightarrow WF_4 + 4BeF$	I	4000	0.96	0.78

TABLE VI: A CATALOG OF ABLATION REACTIONS (Pressure = 1000 psia) (page 8)

Corrodant	Principal Reaction	Type	Temp., °K	A	B
	Ablator: W/c (continued)				
CO	$W/c + 2CO \rightarrow WC/c + CO_2$	III	2000	0.10	0.10
CO	$W/c + 2CO \rightarrow WC/c + CO_2$	III	3000	0.0032	0.0032
CO	$W/c + 2CO \rightarrow WC/c + CO_2$	III	4000	0.0001	0.0001
CO_2	$3W/c + 9CO_2 \rightarrow W_3O_9 + 9CO$	I	2000	1.3	---
CO_2	$3W/c + 9CO_2 \rightarrow W_3O_9 + 9CO$	I	3000	1.12	1.06
CO_2	----------	---	4000	1.23	1.25
HCl	$2W/c + 10HCl \rightarrow 2WCl_5 + 5H_2$	I	2000	0.056	0.056
HCl	$2W/c + 10HCl \rightarrow 2WCl_5 + 5H_2$	I	3000	0.023	0.021
HCl	$W/c + 2HCl \rightarrow WCl_2 + H_2$	I	4000	0.021	0.021
HF	$W/c + 4HF \rightarrow WF_4 + 2H_2$	I	2000	1.67	1.40
HF	$W/c + 4HF \rightarrow WF_4 + 2H_2$	I	3000	1.30	1.17
HF	$W/c + 4HF \rightarrow WF_4 + 2H_2$	I	4000	1.07	1.03
LiF	$W/c + 4LiF \rightarrow WF_4 + 4Li$	I	4000	0.085	0.080

3.4 ANALYTICAL SOLUTIONS FOR TYPICAL CASES AND COMMENTS

3.4.1 MATHEMATICAL DEVELOPMENTS

Mathematical treatments are presented in the following (Case I, Case II, Case III and Case IV) to show how isothermal saturation numbers for typical ablation reactions with inert diluents are determined for each of the four main classes.

Case I: No change in gaseous moles

Reaction: $X/c + Y \overset{K}{\rightleftharpoons} XY$ (1)

Assume: X/c is essentially non-volatile.
Gaseous component Z is inert.

a. For pure Y in feed:

$$p_Y = \left(\frac{1}{K+1}\right)\pi \quad (2)$$

$$p_{XY} = \left(\frac{K}{K+1}\right)\pi \quad (3)$$

and

$$A_Y = \left(\frac{K}{K+1}\right)\left(\frac{M_X}{M_Y}\right) \quad (4)$$

b. For mixture of Y and Z in feed:

$$[1 \text{ mole feed} = f \text{ moles } Y + (1-f) \text{ moles } Z] \quad (5)$$

$$p_Y = \left(\frac{1}{K+1}\right) f\pi \quad (6)$$

$$p_{XY} = \left(\frac{K}{K+1}\right) f\pi \quad (7)$$

$$p_Z = (1-f)\pi \quad (8)$$

and $$A_{Y+Z} = \frac{\left(\frac{K}{K+1}\right) f M_X}{f M_Y + (1-f) M_Z} \quad (9)$$

or

$$A_{Y+Z} = \left[\frac{f M_Y}{f M_Y + (1-f) M_Z}\right] A_Y \quad (10)$$

or, in other words

$$\left(\frac{A_{Y+Z}}{A_Y}\right) = \left(\frac{\text{weight Y in feed}}{\text{total weight feed}}\right) \quad (11)$$

showing the linear relation for additivity when no mole change is involved.

c. For mixture of Y and XY in feed:

$$[1 \text{ mole feed} = f \text{ moles } Y + (1-f) \text{ moles } XY] \quad (12)$$

$$p_Y = \left(\frac{1}{K+1}\right)\pi \quad (13)$$

$$p_{XY} = \left(\frac{K}{K+1}\right)\pi \quad (14)$$

Assume that $\left(\frac{K}{K+1}\right) > (1-f)$, i.e., A_{Y+XY} positive:

Then $$A_{Y+XY} = \frac{\left[\left(\frac{K}{K+1}\right) - (1-f)\right] M_X}{M_Y + (1-f) M_X} \quad (15)$$

or

$$A_{Y+XY} = \frac{\left[\left(\frac{K}{K+1}\right) - (1-f)\right] M_X}{f M_Y + (1-f) M_{XY}} \quad (16)$$

or in other words,

$$A_{Y+XY} = \frac{1}{f}\left[A_Y - (1-f)\left(\frac{M_X}{M_Y}\right)\right]\left(\frac{\text{weight Y in feed}}{\text{total weight feed}}\right) \quad (17)$$

where $\frac{1}{f}\left[A_Y - (1-f)\left(\frac{M_X}{M_Y}\right)\right]$ is always less than A_Y

In this case although there is no change in moles on reaction, the simple additivity rule would fail.

Case II: Increase in gaseous moles

Reaction: $X/c + WY \underset{}{\overset{K}{\rightleftharpoons}} W + XY$ (1)

Assume: X/c is essentially non-volatile.

Gaseous component Z is inert.

a. For pure WY in feed:

$$p_{WY} = \pi - 2K\left(-1 + \sqrt{1 + \frac{\pi}{K}}\right) \quad (2)$$

$$p_{XY} = p_W = K\left(-1 + \sqrt{1 + \frac{\pi}{K}}\right) \quad (3)$$

and $$A_{WY} = \left[\frac{K\left(-1 + \sqrt{1 + \frac{\pi}{K}}\right)}{\pi - K\left(-1 + \sqrt{1 + \frac{\pi}{K}}\right)}\right]\left(\frac{M_X}{M_Y}\right) \quad (4)$$

b. For mixture of WY + Z in feed:

$$[1 \text{ mole feed} = f \text{ moles } WY + (1-f) \text{ moles } Z] \quad (5)$$

$$p_{WY} = f\pi - K\left(\frac{1+f}{2}\right)\left[-(1+f) + \sqrt{(1+f)^2 + 4f\left(\frac{\pi}{K}\right)}\right] \quad (6)$$

$$p_{XY} = p_W = \left(\frac{K}{2}\right)\left[-(1+f) + \sqrt{(1+f)^2 + 4f\left(\frac{\pi}{K}\right)}\right] \quad (7)$$

$$p_Z = (1-f)\left\{\pi - \left(\frac{K}{2}\right)\left[-(1+f) + \sqrt{(1+f)^2 + 4f\left(\frac{\pi}{K}\right)}\right]\right\} \quad (8)$$

and

$$A_{WY+Z} = \frac{\left(\frac{K}{2}\right)\left[-(1+f) + \sqrt{(1+f)^2 + 4f\left(\frac{\pi}{K}\right)}\right] M_X}{\left\{\pi - \left(\frac{K}{2}\right)\left[-(1+f) + \sqrt{(1+f)^2 + 4f\left(\frac{\pi}{K}\right)}\right]\right\}\left[f M_{WY} + (1-f) M_Z\right]} \quad (9)$$

or

$$A_{WY+Z} = \left[\frac{f M_{WY}}{f M_{WY} + (1-f) M_Z}\right] A'_{WY} \tag{10}$$

or

$$A_{WY+Z} = \left(\frac{\text{weight WY in feed}}{\text{total weight feed}}\right) A'_{WY} \tag{11}$$

where

$$A'_{WY} = \frac{\left(\frac{K}{2}\right)\left[-(1+f)+\sqrt{(1+f)^2+4f\left(\frac{\pi}{K}\right)}\right]}{f\left\{\pi-\left(\frac{K}{2}\right)\left[-(1+f)+\sqrt{(1+f)^2+4f\left(\frac{\pi}{K}\right)}\right]\right\}}\left(\frac{M_X}{M_{WY}}\right) \tag{12}$$

$$\text{But } A'_{WY} \neq A_{WY} \tag{13}$$

Given:

$$A_{WY} = \frac{\left[-1+\sqrt{1+\left(\frac{\pi}{K}\right)}\right]}{\left\{\left(\frac{\pi}{K}\right)-\left[-1+\sqrt{1+\left(\frac{\pi}{K}\right)}\right]\right\}}\left(\frac{M_X}{M_{WY}}\right) \tag{14}$$

and

$$A'_{WY} = \frac{\left(\frac{1}{2}\right)\left[-(1+f)+\sqrt{(1+f)^2+4f\left(\frac{\pi}{K}\right)}\right]}{f\left\{\left(\frac{\pi}{K}\right)-\left(\frac{1}{2}\right)\left[-(1+f)+\sqrt{(1+f)^2+4f\left(\frac{\pi}{K}\right)}\right]\right\}}\left(\frac{M_X}{M_{WY}}\right) \tag{15}$$

Then:

$$\frac{A'_{WY}}{A_{WY}} = \frac{\left(\frac{1}{2}\right)\left[-(1+f)+\sqrt{(1+f)^2+4f\left(\frac{\pi}{K}\right)}\right]}{\left[-1+\sqrt{1+\left(\frac{\pi}{K}\right)}\right]}$$

$$\times \frac{\left\{\left(\frac{\pi}{K}\right)-\left[-1+\sqrt{1+\left(\frac{\pi}{K}\right)}\right]\right\}}{f\left\{\left(\frac{\pi}{K}\right)-\left(\frac{1}{2}\right)\left[-(1+f)+\sqrt{(1+f)^2+4f\left(\frac{\pi}{K}\right)}\right]\right\}} \tag{16}$$

Given $\left(\frac{\pi}{K}\right)$, one can plot $\frac{A'_{WY}}{A_{WY}}$ vs. f.

$$\text{At } f \cong 1,\ \frac{A'_{WX}}{A_{WY}} \cong 1 \tag{17}$$

$$\text{At } f \cong 0,\ \frac{A'_{WX}}{A_{WY}} \cong \frac{\left(\frac{M_X}{M_{WY}}\right)}{A_{WY}} \tag{18}$$

$$\left[\text{ or } A'_{WY} \cong \frac{M_X}{M_{WY}}\right] \tag{19}$$

$$\text{In range } f = 0 \text{ to } f = 1,\ \frac{A'_{WX}}{A_{WY}} > 1 \tag{20}$$

c. For mixtures of WY + W, or WY + XY in feed:

(This case not derived.)

Case III: Decrease in gaseous moles.

Reaction: $X/c + 2Y \overset{K}{\rightleftharpoons} XY_2$ (1)

Assume: X/c is essentially non-volatile.

Gaseous component Z is inert.

a. For pure Y feed:

$$p_Y = \left(\frac{-1+\sqrt{1+4K\pi}}{2K}\right) \tag{2}$$

$$p_{XY_2} = \pi - \left(\frac{-1+\sqrt{1+4K\pi}}{2K}\right) \tag{3}$$

and $$A_Y = \left(\frac{1+2K\pi-\sqrt{1+4K\pi}}{1+4K\pi-\sqrt{1+4K\pi}}\right)\left(\frac{M_X}{M_Y}\right) \tag{4}$$

b. For mixture of Y and Z in feed:

$$[1 \text{ mole feed} = f \text{ moles } Y + (1-f) \text{ moles } Z] \tag{5}$$

$$p_Y = \frac{-1+\sqrt{1+4f(2-f)K\pi}}{2(2-f)K} \tag{6}$$

$$p_{XY_2} = \frac{[1+2f(2-f)K\pi]-\sqrt{1+4f(2-f)K\pi}}{2(2-f)^2K} \tag{7}$$

$$p_Z = (1-f)\left\{\frac{[1+4(2-f)K\pi]-\sqrt{1+4f(2-f)K\pi}}{2(2-f)^2K}\right\} \tag{8}$$

and

$$A_{Y+Z} = \left\{\frac{[1+2f(2-f)K\pi]-\sqrt{1+4f(2-f)K\pi}}{[1+4(2-f)K\pi]-\sqrt{1+4f(2-f)K\pi}}\right\}\left[\frac{M_X}{fM_Y+(1-f)M_Z}\right] \tag{9}$$

or

$$A_{Y+Z} = \left[\frac{fM_Y}{fM_Y + (1-f)M_Z}\right]A'_Y \tag{10}$$

or

$$A_{Y+Z} = \left(\frac{\text{weight Y in feed}}{\text{total weight feed}}\right)A'_Y \tag{11}$$

where (12)

$$A'_Y = \left[\frac{[1 + 2f(2-f)K\pi] - \sqrt{1 + 4f(2-f)K\pi}}{f\{[1 + 4(2-f)K\pi] - \sqrt{1 + 4f(2-f)K\pi}\}}\right]\left(\frac{M_X}{M_Y}\right)$$

But $A'_Y \neq A_Y$ (13)

$$\frac{A'_Y}{A_Y} = \left\{\frac{[1 + 2f(2-f)K\pi] - \sqrt{1 + 4f(2-f)K\pi}}{[1 + 2K\pi] - \sqrt{1 + 4K\pi}}\right\}$$

$$X\left[\frac{[1 + 4K\pi] - \sqrt{1 + 4K\pi}}{f\{[1 + 4(2-f)K\pi] - \sqrt{1 + 4f(2-f)K\pi}\}}\right] \tag{14}$$

Given $K\pi$, one can plot $\frac{A'_Y}{A_Y}$ vs. f.

$$\text{At } f \cong 1, \frac{A'_Y}{A_Y} \cong 1 \tag{15}$$

$$\text{At } f \cong 0, \frac{A'_Y}{A_Y} \cong 0 \tag{16}$$

$$[\text{or } A'_Y \cong 0] \tag{17}$$

$$\text{In range } f = 0 \text{ to } f = 1, \frac{A'_Y}{A_Y} < 1 \tag{18}$$

c. For mixture of Y and XY_2 in feed:

(This case not derived.)

Case IV: Inert gas feed; simple decomposition of ablator.

Reaction: $X/c \rightleftharpoons X$ (1)

Assume Z_1 and Z_2 are inert.

a. Feed composition: 1 mole feed = f moles Z_1 and (1-f) moles Z_2. (2)

$$p_X = K \tag{3}$$

$$p_{Z_1} = f(\pi - K) \tag{4}$$

$$p_{Z_2} = (1-f)(\pi - K) \tag{5}$$

$$A_{Z_1+Z_2} = \frac{K M_X}{(\pi - K)[f M_{Z_1} + (1-f) M_{Z_2}]} \tag{6}$$

But $$A_{Z_1} = \left(\frac{K}{\pi - K}\right)\left(\frac{M_X}{M_{Z_1}}\right) \tag{7}$$

$$A_{Z_2} = \left(\frac{K}{\pi - K}\right)\frac{M_X}{M_{Z_2}} \tag{8}$$

Thus $$A_{Z_1+Z_2} = \frac{A_{Z_1} A_{Z_2}}{f A_{Z_2} + (1-f) A_{Z_1}} \tag{9}$$

or

$$A_{Z_1+Z_2} = A_{Z_1}\left(\frac{\text{weight } Z_1 \text{ in feed}}{\text{total weight feed}}\right) + A_{Z_2}\left(\frac{\text{weight } Z_2 \text{ in feed}}{\text{total weight feed}}\right) \tag{10}$$

The additivity rule applies in this case, even though there is a change in gaseous moles.

b. Feed composition: X + inert.

(This case not derived.)

3.4.2 COMMENTS

It is seen that the simple additivity rule applies only for reactions involving zero mole change, or for ablator decomposition reactions with inert diluents. For reactions involving an increase in gaseous moles, equilibrium ablation, as would be expected, is enhanced by either a drop in total pressure or dilution with inerts; exactly the reverse is true for reactions in which net gaseous moles disappear. As part of Case I, it is also shown that dilution with an ablation product species reverses the corrosion equilibria, yielding lower isothermal saturation numbers than dilution with a comparable amount of inerts. The same should hold true for the other three cases as well.

Within certain limitations, the method may be extended to cover other situations as well. For reactions having mole changes such as $2 \rightarrow 3$, $1 \rightarrow 3$, or $1 \rightarrow 4$, rigorous mathematical treatment becomes unwieldy, since a third-or-higher order algebraic equation must be solved. It is obvious. from extension of Case I, that the "additivity"rule still applies to two or more independent ablation reactions, if the mole change is zero for each. If the mole changes are not zero, the problem of two independent reactions is much more complex. Fortunately, one ablation equilibrium usually predominates over the others in mixtures of practical interest.

3.5 EXAMPLES

Two examples are provided to illustrate the application of the method, and to point out some calculational details not apparent from the preceding discussion. The first system involves BOF as the major corrodant, while in the second case, H_2 is the principal reacting species. In both examples the ablator is graphite (C/c).

Example 1: $T_c = 3865^{\circ}K$, $P_c = 500$ psia, C-H-N-O-F-B propellant.

The computer-derived equilibrium composition of the free stream at the given temperature and pressure was recalculated in terms of the minimum number of stable species required to make up the system at these conditions. Since the isothermal saturation number "A" is fixed by overall equilibrium rather than by reaction rates, this simplification appears a valid means of eliminating minor or uncertain species from consideration. For the system under consideration, the composition was most conveniently expressed in terms of the following: BF, BOF, CO, HF, H_2, N_2.

	Composition		A_{1000}, Isothermal Saturation Number at 1000 psia
	Gm-moles 100 gms	Gms 100 gms	
BF	0.050	1.49	0*
BOF	0.872	39.93	0.27
CO	1.286	36.02	0.0035
HF	0.021	0.42	0.17
H_2	0.088	0.18	5.0
N_2	0.784	21.96	0.072

*Estimated from "A's" of BF_3 and BF_2.

On preliminary examination, the major corrodant species is seen to be BOF, based on both its "A" value at 1000 psia, and upon its large weight fraction. (H_2 has a much higher value of "A", but based upon its very small weight fraction, should not be a significant reactant.) The ablation reaction of BOF with graphite is:

$$C/c + BOF \overset{K_1}{\rightleftharpoons} CO + BF$$

This equation fits the form of Case II:

$$X/c + WY \overset{K}{\rightleftharpoons} W + XY \qquad \text{(Eq. II-1)}$$

in which X is C, W is BF, and Y is O. The equilibrium constant, "K_1", may be obtained from the JANAF thermochemical data tables, or, as an alternative, evaluated from the computed "A" value for BOF at 3865°K. In order to allow for the effects of minor side reactions, the latter is preferable:

$$0.27 \cong \frac{-1 + \sqrt{1 + \left(\frac{68.0}{K_1}\right)}}{\left(\frac{68.0}{K_1}\right) - \left[-1 + \sqrt{1 + \left(\frac{68.0}{K_1}\right)}\right]} \left(\frac{12.01}{45.82}\right) \qquad \text{(Eq. II-4)}$$

from which $K_1 \cong \infty$; i.e., the ablation reaction goes essentially to completion.

Knowing that the "A" value for BOF is determined by stoichiometry rather than by equilibrium, the approach must be modified as follows:

(1) The value A = 0.27 for BOF at 3865°K can be assumed constant, irrespective of the total pressure or the dilution.

(2) The influence of the large CO concentration on the BOF ablation reaction can be neglected.

(3) Since the BOF stoichiometry is fixed, some other species can be considered as a major corrodant.

The next most corrosive species is seen to be N_2, by virtue of the reaction:

$$2C/c + N_2 \overset{K_2}{\rightleftharpoons} 2CN$$

The equation also fits the form of Case II:

$$X/c + WY \overset{K}{\rightleftharpoons} W + XY \qquad \text{(Eq. II-1)}$$

in which X is 2C, W is CN, and Y is $C^{-1}N$.

As before, the equilibrium constant, "K_2", may be evaluated from the computed value of "A" at 3865°K and 1000 psia:

$$0.072 = \frac{-1 + \sqrt{1 + \left(\frac{68.0}{K_2}\right)}}{\left(\frac{68.0}{K_2}\right) - \left[-1 + \sqrt{1 + \left(\frac{68.0}{K_2}\right)}\right]} \left(\frac{24.02}{28.02}\right) \qquad \text{(Eq. II-4)}$$

from which $K_2 \cong 0.49$. At 500 psia pressure and 3865°K, the "A" value for pure N_2 attacking graphite would be:

$$A_{500} \cong \frac{-1 + \sqrt{1 + \left(\frac{34.0}{0.49}\right)}}{\left(\frac{34.0}{0.49}\right) - \left[-1 + \sqrt{1 + \left(\frac{34.0}{0.49}\right)}\right]} \left(\frac{24.02}{28.02}\right) = 0.102^* \qquad \text{(Eq. II-4)}$$

(*This computation shows how the method can be used to compute total pressure effects but is not otherwise used in the material which follows.)

In the given mixture, the mole fraction of N_2 is 0.252. Accordingly, the "effective" isothermal saturation number of N_2 in the mixture may be derived:

$$A'_{500} \cong \frac{\frac{1}{2}\left[-1.252 + \sqrt{(1.252)^2 + (4)(0.252)\left(\frac{34.0}{0.49}\right)}\right]}{0.252\left\{\left(\frac{34.0}{0.49}\right) - \frac{1}{2}\left[-1.252 + \sqrt{(1.252)^2 + (4)(0.252)\left(\frac{34.0}{0.49}\right)}\right]\right\}} \left(\frac{24.02}{28.02}\right) = 0.217$$

(Eq. II-15)

Neglecting effects of pressure and dilution upon the ablation equilibria for the minor corrodant species, the overall "A" value for the combustion mixture at 3865°K and 500 psia can be estimated:

$$A \cong \Big[(1.49)(0) + (39.93)(0.27) + (36.02)(0.0035) + (0.42)(0.17) + (0.18)(5.0) + (21.96)(0.217)\Big] \div 100 = 0.166$$

This compares to an "A" value of 0.168 determined rigorously, using an IBM 7090 computer.

Example 2: $T_c = 2793^{\circ}K$, $P_c = 1000$ psia, B-N-H propellant

As in Example 1, the computed equilibrium composition was recalculated in terms of the minimum number of stable species. For the system under consideration, the composition was expressed in terms of H_2, N_2, and BN/c:

	Composition		A_{1000}, Isothermal Saturation Number at 1000 psia
	Gm-moles 100 gms	Gms 100 gms	
H_2	6.609	13.32	0.44
N_2	0.165	4.62	0.0009
BN/c	3.305	82.06	0*

(*Assumed non-reactive.)

Since BN/c was considered inert, calculations were based only on the gas phase.

The major corrodant species is seen to be H_2. At this temperature and pressure, the primary ablation reaction of H_2 with graphite is:

$$2C/c + H_2 \overset{K}{\rightleftharpoons} C_2H_2$$

This equation fits the form of Case I:

$$X/c + Y \overset{K}{\rightleftharpoons} XY \qquad \text{(Eq. I-1)}$$

in which X is 2C and Y is H_2.

Because the reaction involves no change in gaseous moles, dilution effects can be neglected.

The isothermal saturation number of only the gas phase may be estimated:

$$A_{gas} \cong \frac{(13.32)(0.44) + (4.62)(0.0009)}{(13.32) + (4.62)} = 0.327$$

Based upon the total combustion mixture, the isothermal saturation number would be predicted as:

$$A \cong \frac{(13.32)(0.44) + (4.62)(0.0009) + (82.06)(0)}{100} = 0.059$$

This compares to an "A" value of 0.079 determined rigorously, using an IBM 7090 computer. In this instance, the method does not give as good an estimate of "A", as desired.

By inspection of the computed equilibrium composition of the combustion mixture after saturation with graphite, the reason for the discrepancy between predicted and computed "A" values was uncovered. A major product of the ablation process was found to be gaseous HCN, which obviously was not taken into account in the individual "A" values of H_2 and N_2 with C/c considered separately. Owing to a three-way chemical interaction between two combustion species and the ablator, the prediction approach breaks down in this case.

SECTION 4

PLANS FOR FUTURE WORK

It is contemplated that future effort under this contract will be devoted to the following:

(1) Detailed study of HfN, the highest melting nitride, in equilibrium with various "pure" gases.

(2) Interpretation of computer results to compare suitability of various materials in various atmospheres, considering melting points and density effects. The degree of cooling $\left[(T_{\text{free stream}} - T_{\text{wall}})/B \right]$ per unit of wall material evaporated or in other fashion will be considered.

(3) Comparison of various materials for real propellants.

(4) Comparison of theoretical corrosion rate predictions against measured values for real propellants or pure gases.

Certain other areas such as solid (or liquid)-solid reactions, effects of uncertainties in thermodynamic data, further mixture and pressure effects, and a general study of other types of materials will be carried out as time permits.

REFERENCES

1. Stephanou, S. E., Oliver, R. C. and Baier, R. W., "Chemical Corrosion of Rocket Liner Materials and Propellant Performance Studies," Second Quarterly Report, Vol. I of III, 15 December 1962, Contract NOw 61-0905-C, Task E.

2. Oliver, R. C. and Baier, R. W., Ibid, Third Quarterly Report, 15 March 1963.

3. JANAF Interim Thermochemical Tables, The Dow Chemical Company, Midland, Michigan.

4. Chao, Jing, Private Communication, Dow Chemical Company, April 30, 1963.

5. Hildenbrand, D. L., Aeronutronic Division, Ford Motor Company, Newport Beach, Private Communication.

6. Ackermann, R. J. and Thorn, R. J., "Vaporization of Oxides," in Progress in Ceramic Science, Vol. 1, J. E. Burke, Editor, Pergamon Press, Oxford, 1961.

7. NBS 500, "Selected Values of Chemical Thermodynamic Properties."

8. Ackermann, R. J., Rauk, E. G., Thorn, R. J. and Cannon, M. C., J. Chem. Phys., 67, 762 (1963).

APPENDIX

ERRATA IN PREVIOUS REPORTS

A number of significant errors or omissions in presentation have been noted in the three previous quarterlies issued under this contract, as follows:

First Quarterly (15 September, 1962)

p. 16 -- N_x^c should be defined as moles of nozzle material as condensed phase per 100 grams of equilibrium mixture, including condensed phase.

p. 17 and Figures 1-8 -- the pressure used in these calculations was 1000 psia.

Second Quarterly (15 December, 1962) - Volume I

p. 66 -- ΔH^o_{f298} for $WF_5(g)$ should be listed as -384 kcal/mole.

Third Quarterly (15 March, 1963)

p. 4 -- Brackets should surround the terms following T, as

$$\left[H_T - H_{298} - Cp_{298}\,(T-298)\right]$$

p. 6 -- The symbol identification code should read

- o Southern Research
- □ Mezaki
- x K. K. Kelley

p. 33 -- The title for Figure 9 should have the words "at 1000 psia" added.

p. 36 -- The title of the referenced publication should read "Thermodynamic Properties of Inorganic Substances, V. High Temperature Heat Contents of Fifteen Refractory Borides."